Autonomous and nonautonomous roles of Hedgehog signaling in regulating limb muscle formation

Jimmy Kuang-Hsien Hu, Edwina McGlinn, Brian D. Harfe, et al.

Genes Dev. 2012 26: 2088-2102
Access the most recent version at doi:10.1101/gad.187385.112

Autonomous and nonautonomous roles of Hedgehog signaling in regulating limb muscle formation

Jimmy Kuang-Hsien Hu,[1] Edwina McGlinn,[1,4] Brian D. Harfe,[2] Gabrielle Kardon,[3] and Clifford J. Tabin[1,5]

[1]Department of Genetics, Harvard Medical School, Boston, Massachusetts 02115, USA; [2]Department of Molecular Genetics and Microbiology, The Genetics Institute, University of Florida, Gainesville, Florida 32610; [3]Department of Human Genetics, University of Utah, Salt Lake City, Utah 84112, USA

Muscle progenitor cells migrate from the lateral somites into the developing vertebrate limb, where they undergo patterning and differentiation in response to local signals. Sonic hedgehog (Shh) is a secreted molecule made in the posterior limb bud that affects patterning and development of multiple tissues, including skeletal muscles. However, the cell-autonomous and non-cell-autonomous functions of Shh during limb muscle formation have remained unclear. We found that Shh affects the pattern of limb musculature non-cell-autonomously, acting through adjacent nonmuscle mesenchyme. However, Shh plays a cell-autonomous role in maintaining cell survival in the dermomyotome and initiating early activation of the myogenic program in the ventral limb. At later stages, Shh promotes slow muscle differentiation cell-autonomously. In addition, Shh signaling is required cell-autonomously to regulate directional muscle cell migration in the distal limb. We identify *neuroepithelial cell transforming gene 1* (*Net1*) as a downstream target and effector of Shh signaling in that context.

[*Keywords*: Shh; Smo; limb muscles; Net1; cell migration]

Supplemental material is available for this article.

Received January 20, 2012; revised version accepted May 29, 2012.

Developmentally, the vertebrate limb is a mosaic structure wherein some cell types, such as the skeletal and connective tissues, arise from the lateral plate-derived limb mesenchyme (Dhouailly and Kieny 1972; Chevallier et al. 1977), while others, such as the muscles and some endothelial cells, are derived from the somites (Christ et al. 1977; Kardon et al. 2002; Huang et al. 2003; Bryson-Richardson and Currie 2008; Hutcheson et al. 2009). In spite of their disparate origins, once in the limb bud, the progenitors of those tissues respond to the same signaling environment that patterns the limb and orchestrates its morphogenesis. For example, Sonic hedgehog (Shh) is a key signaling molecule expressed in the zone of polarizing activity (ZPA) in the posterior of the vertebrate limb bud from embryonic day 9.75 (E9.75) through E12.5 (Echelard et al. 1993; Riddle et al. 1993; Kruger et al. 2001). Shh protein has also been detected in the limb ectoderm (Bouldin et al. 2010). Functionally, Shh activity is both necessary and sufficient to establish the anterior–posterior (AP) pattern of the limb. Ectopic expression of the Shh at the anterior margin of the chick limb bud results in a mirror-image duplication of all of the tissues of the limb (Riddle et al. 1993), while removal of *Shh* in mice results in a loss of posterior pattern and the development of a single anterior digit (Chiang et al. 2001). However, within the limb bud, which tissues are directly affected by Shh signaling and which tissues are indirectly patterned have not been previously examined.

Shh appears to play multiple sequential roles in regulating the process of myogenesis. The myogenic precursor cells that populate the limb bud originate in the somites (Chevallier et al. 1977; Christ et al. 1977). Shh, produced in the midline by the notochord and the floor plate of the neural tube, is required to activate expression of myogenic determination genes such as *Myf5* and *MyoD* in the epaxial portion of the somite (Münsterberg et al. 1995; Borycki et al. 1999; Gustafsson et al. 2002; McDermott et al. 2005), which gives rise to the deep back muscles. The hypaxial muscle precursors of the dermomyotome are not affected at this stage (Borycki et al. 1999).

The hypaxial cells, including the future limb muscle progenitors, express the paired domain transcription factor Pax3, which is initially expressed throughout the presomitic mesoderm but later becomes restricted to the

[4]Present address: EMBL Australia, Australian Regenerative Medicine Institute, Monash University, Clayton, Victoria 3800, Australia.
[5]Corresponding author
E-mail tabin@genetics.med.harvard.edu
Article is online at http://www.genesdev.org/cgi/doi/10.1101/gad.187385.112.

dermomyotome (Goulding et al. 1991; Williams and Ordahl 1994). At E9.5 in mice or Hamburger and Hamilton stage 17 (HH17) in chicks, myogenic cells start to delaminate from the ventrolateral lip of the dermomyotome and migrate into the forelimb bud to where the dorsal and ventral muscle masses will form initially (Tajbakhsh and Buckingham 2000; Francis-West et al. 2003; Otto et al. 2006). The same process occurs slightly later in the hindlimb. During migration, muscle progenitor cells continue to proliferate and express *Pax3* until arriving in the limb bud and differentiating to become myoblasts, concomitant with the expression of *Myf5* and *MyoD* (Birchmeier and Brohmann 2000; Pownall et al. 2002).

This myogenic differentiation is integrated with the process of pattern formation such that as the muscle cells differentiate and begin to form muscle bundles, they do so in the correct location and orientation (Kardon 1998; Kardon et al. 2003; Li et al. 2010). The AP organization of the muscles is established in response to Shh activity. When Shh is applied to the anterior chick limb bud, anterior muscles are transformed into muscles with posterior identity, in concert with other tissues (Duprez et al. 1999). This is likely an indirect response to Shh, as the patterning of the limb muscles appears to be controlled by the prepattern of the muscle connective tissue (Kardon et al. 2003; Hasson et al. 2010). However, in addition to patterning changes, ectopic Shh also results in an expansion of the *Pax3*-expressing muscle precursor population, leading to muscle hypertrophy (Duprez et al. 1998). Furthermore, in the complete loss of Shh activity in mice, there is a total loss of limb musculature, with the exception of a small portion of the dorsal muscle adjacent to the humerus (Kruger et al. 2001). Explant cultures suggest that this may be due to a requirement for Shh to maintain the expression of *Myf5* and *MyoD* (Kruger et al. 2001).

Shh has also been shown to regulate terminal differentiation of limb muscles. As the muscles differentiate within the limb, they express different compositions of myosin heavy chain (MyHC) isoforms, which are determinants of myofiber types—fatigue-enduring oxidative slow muscle fibers or force-generating glycolytic fast muscle fibers (Gunning and Hardeman 1991; Schiaffino and Reggiani 1996; Wigmore and Evans 2002). For instance, the soleus is enriched with slow fibers, while the tibialis anterior (TA) is largely composed of fast fibers (Agbulut et al. 2003). These differences enable each muscle to adapt to different physiological and functional demands. It has been reported that excessive Shh promotes the formation of slow fibers, while loss of Shh signaling reduces slow muscle fiber formation, due to precocious differentiation (Cann et al. 1999; Bren-Mattison and Olwin 2002; Li et al. 2004).

To attempt to distinguish whether these various effects of Shh on limb muscle development are direct or indirect, we took a genetic approach in mice. *Smoothened (Smo)* encodes a seven-pass transmembrane protein that acts downstream from the Shh receptor Patched and is required for Shh signaling (Alcedo et al. 1996; van den Heuvel and Ingham 1996; Zhang et al. 2001). While *Smo* is required for all hedgehog signaling, Shh is the only member of the Hh family expressed during the early steps of limb development (Echelard et al. 1993; Yang et al. 1998). Thus, by removing *Smo* tissue specifically from the muscle cell precursors or from the surrounding lateral plate-derived mesenchyme, we are able to dissect the cell-autonomous and non-cell-autonomous functions of Shh signaling during limb muscle development. We found that Shh acts non-cell-autonomously to pattern limb musculature through lateral plate-derived tissues. However, Hh signaling is required cell-autonomously to maintain cell survival in the dermomyotome, initiate prompt and robust early *Myf5* and *MyoD* expression in the ventral limb muscle mass, and, at a later stage, promote slow muscle fiber formation in the limb. In addition, Shh signaling is essential for the maintenance of *neuroepithelial cell transforming gene 1* (*Net1*) expression in the myogenic precursors, which in turn regulates directional muscle cell migration in the distal limb.

Results

Shh signaling patterns limb muscles non-cell-autonomously

In order to define the cell-autonomous and non-cell-autonomous functions of Shh signaling during limb muscle development, we removed the ability to respond to Shh signaling specifically from the somite or lateral plate-derived limb mesenchyme by using a conditional allele of *Smoothened* (*Smo*^{fl}) (Long et al. 2001) in conjunction with *Pax3*^{Cre} (Engleka et al. 2005) or *Prx1*^{Cre} (Logan et al. 2002), which encode Cre-recombinases that are expressed in these tissues, respectively. In some crosses, the *Smo*^{fl} allele was combined with a null allele of the gene *Smo*^{del}. *Smo*$^{del/+}$ did not show any phenotype. We first examined the cell-autonomous role of Shh signaling during the AP patterning of the forelimb muscles by creating either *Pax3*^{Cre}; *Smo*$^{fl/fl}$ or *Pax3*^{Cre}; *Smo*$^{fl/del}$ embryos [collectively referred to as *Pax3*^{Cre}; *Smo*$^{CKO\ (conditional\ knockout)}$ when giving the same phenotype]. At E12.5, *MyoD* whole-mount in situ hybridization revealed a loss of *MyoD* expression in the cervical somites (Supplemental Fig. 1B). In regions where *MyoD* was expressed, the mutant myotomes were shorter than those of the wild-type *Pax3*^{Cre}; *Smo*$^{fl/+}$ siblings (Supplemental Fig. 1A,B). They had additionally lost parts of the epaxial dermomyotome (Supplemental Fig. 1C,D), a phenotype that was also seen in the *Shh*$^{-/-}$ mutants (Borycki et al. 1999), presumably due to an inability to respond to the midline Shh. However, AP patterning in the mutant proximal limb muscles was unaffected, although the *MyoD*-expressing domain appeared to be reduced in size at E12.5 (Fig. 1C). This decrease in *MyoD* expression did not affect the eventual muscle mass and patterning, as supported by immunostaining at E16.5 using an antibody against smooth muscle actin (SMA) (Fig. 1D,F), which is expressed in the skeletal muscles at this stage (Supplemental Fig. 2A–B″). In these mutants, Pax3-Cre recombinase effectively led to recombination in the somites and all limb muscles but not in the lateral plate-derived tissues, hence enabling removal of Hh

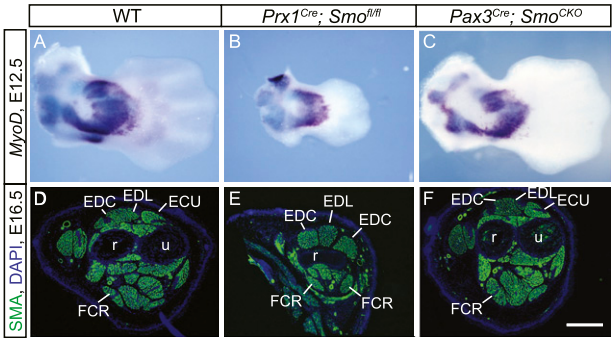

Figure 1. Shh signaling patterns limb muscle non-cell-autonomously. (*A–C*) *MyoD* expression of mouse forelimbs was analyzed by whole-mount in situ hybridization at E12.5 (dorsal views). (*D–F*) The expression of SMA was detected by immunostaining at E16.5 (transverse sections). While the forelimb muscles of wild-type (WT) embryos were correctly patterned along the AP axis (*A*,*D*), AP patterning was lost in the mutant forelimb muscles, where Shh activity was removed in the nonmuscle limb mesenchyme (*B*,*E*). (*C*,*F*) Cell-autonomous removal of Shh activity in the muscles did not affect AP patterning. (ECU) Extensor carpi ulnaris; (EDC) extensor digitorum communis; (FCR) flexor carpi radialis; (r) radius; (u) ulna. Bar in *F*: *A–C*, 480 μm; *D–F*, 400 μm.

signaling specifically in the myogenic cells (Table 1; Supplemental Fig. 2C–D″,G,H). These data show that Shh does not pattern the proximal limb muscles cell-autonomously. While no proximal patterning changes were observed, we did note a complete loss of muscle tissue in the distal-most limb, a phenotype analyzed below.

To verify that the patterning of the limb muscles by Shh is an indirect, nonautonomous effect, we specifically removed the ability of the nonmuscle cells of the limb to respond to Shh, while leaving Shh signal transduction intact in the myogenic populations. To this end, we generated $Prx1^{Cre}$; $Smo^{fl/fl}$ embryos where $Prx1^{Cre}$ is only active in the lateral plate-derived tissues (Supplemental Fig. 2E–F″). $Prx1^{Cre}$; $Smo^{fl/fl}$ embryos exhibited a Shh mutant-like limb phenotype with a much shortened limb and reduced posterior skeletal elements. Limb muscles in this mutant appear symmetrical, with an anatomy most consistent with a double anterior pattern along the AP axis (Fig. 1B,E). Therefore, these data do indeed confirm the idea that Shh patterns limb muscles along the AP axis through lateral plate-derived mesenchyme in a non-cell-autonomous manner, consistent with previous work indicating that the pattern of the musculature is established by the muscle connective tissue (Kardon et al. 2003; Hasson et al. 2010; Li et al. 2010).

Hh signaling promotes slow muscle fiber formation cell-autonomously

In addition to its early effect on muscle patterning, memory of Shh exposure could also have an effect on later muscle differentiation. Moreover, the related protein Indian hedgehog (Ihh), produced in the developing cartilage elements, could also influence later muscle development (Bren-Mattison et al. 2011). As Smo is required for both Shh and Ihh activity, its removal will block all Hh signaling in the developing limb. To determine whether Hh signaling is required non-cell-autonomously for the regulation of terminal muscle differentiation at later stages, we used Tcf4-Cre recombinase (encoded by $Tcf4^{GFPCre+neo}$) to remove *Smo* from muscle connective tissue, which arises from the lateral plate-derived limb mesenchyme and has previously been reported to regulate muscle fiber type (Mathew et al. 2011). However, $Tcf4^{GFPCre+neo}$; $Smo^{fl/fl}$ mutant embryos appeared to be normal in both connective tissue and muscle patterning and differentiation (Supplemental Fig. 1E,F; data not shown). Slow muscle fiber formation is a hallmark of limb muscle terminal differentiation and can be detected by using an antibody against myosin heavy chain I (MyHCI). To study whether terminal differentiation is affected, we therefore quantified the proportion of slow muscle fiber in the soleus and the extensor digitorum longus (EDL) of the hindlimb, which contains a higher proportion of slow muscle fibers than the forelimb and has been traditionally used to examine this aspect of muscle differentiation. However, no changes were observed (Fig. 2D,H).

In contrast, when Hh responsiveness was removed directly from limb muscles in the $Pax3^{Cre}$; Smo^{CKO} mutant embryos, there was a significant decrease in the percentage of slow muscle fiber in the soleus and EDL compared with the wild type at E18.5 (Fig. 2A–C,E–G). This indicates that Hh signaling promotes slow muscle fiber formation in the limb in a cell-autonomous fashion, a mechanism that is analogous to the adaxial slow muscle fiber formation in the zebrafish (Baxendale et al. 2004; Feng et al. 2006). To directly assess whether Shh signaling is capable of regulating differentiation of myogenic limb bud cells, we next performed an in vitro differentiation

Table 1. *Microarray results*

Genes	Ventral muscle mass	*P*-value	Dorsal muscle mass	*P*-value
Smo	16.47	0.019462	9.3	0.028431
Zic1	6.58	0.041054	4.05	0.033232
Tbx1	5.37	0.031714	4.09	0.034367
Net1	4.51	0.013456	3.17	0.02355
Fgf15	4.35	0.039025	4.59	0.036518
Ptch1	4.23	0.019941	2.94	0.026412
Meox2	4.20	0.036276	6.43	0.026385
Pgf	3.90	0.010072	2.28	0.019901
Nkx3-1	3.76	0.007874	2.22	0.023284
Gad1	3.42	0.033169	1.73	0.022986
Pgam2	3.13	0.032728	2.5	0.023923
Scara3	3.05	0.039215	2.61	0.030084
Grb14	2.89	0.013878	1.8	0.013472
Ankrd6	2.79	0.048979	2.42	0.040351
Fzd10	2.57	0.011547	2.06	0.035782
Zic4	2.56	0.039428	1.53	0.060918
Dock9	2.28	0.04883	2.69	0.042133
c-Met	2.15	0.063983	1.87	0.024217

Relative fold decrease of selected genes in the E11.25 $Pax3^{Cre}$; Smo^{CKO}; *RC::rePe* mutant ventral and dorsal limb muscle cells when compared with those of the wild-type siblings. *P*-value was corrected using the Benjamin and Hochberg false discovery rate.

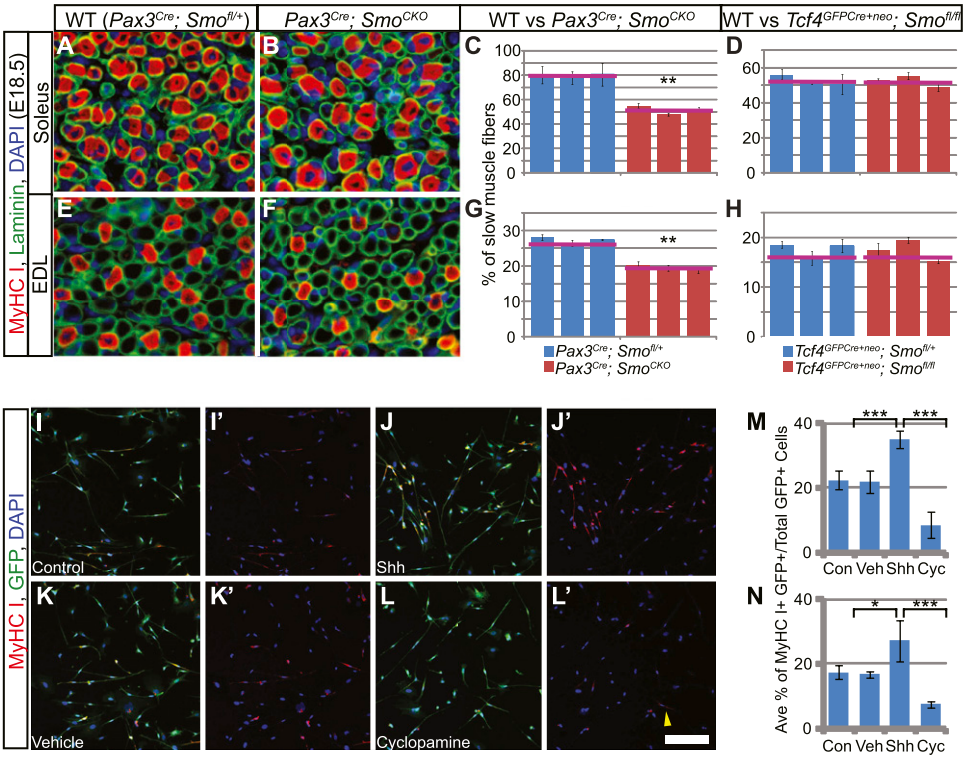

Figure 2. Hh signaling promotes slow muscle fiber formation cell-autonomously. (*A*,*B*,*E*,*F*) Frozen sections from the hindlimb soleus (*A*,*B*) and EDL (*E*,*F*) were immunostained for laminin to mark all muscle fibers and type I myosin to label slow muscle fibers at E18.5. (*C*,*D*,*G*,*H*) The proportion of slow muscle fibers in the soleus (*C*,*D*) and EDL (*G*,*H*) was quantified as previously described (Hutcheson et al. 2009). Slow muscle fibers were found to be decreased in limbs with cell-autonomous removal of Hh signaling (*C*,*G*) but unchanged when Hh signaling was abrogated in muscle connective tissues (*D*,*H*). The red lines mark the average value from all three individuals of the same genotype. (*I*–*L*′) After 7 d of differentiation, hindlimb myogenic cells cultured in the presence of Shh protein exhibited more MyHCI-positive slow myofibers than the control cells (shown in *I*–*J*′). (*L*,*L*′) However, in the presence of cyclopamine, few MyHCI signals were detected, with occasional faintly stained cells (yellow arrowhead). (*K*,*K*′) Vehicle control had no effect on the cells. (*M*,*N*) When quantified, GFP-positive myogenic cells from both the hindlimb (*M*) and forelimb (*N*) showed a significant increase in the proportion of MyHCI slow myofibers when cultured with Shh protein and decreased slow muscle fibers in the presence of cyclopamine. Histograms are expressed as means and standard error of the mean (SEM). (Con) Control; (Veh) vehicle control; (Cyc) cyclopamine. Bar in *L*′: *A*,*B*,*E*,*F*, 20 μm; *I*–*L*′, 200 μm.

assay. To isolate myogenic cells, we generated *Pax3*^{Cre}*; RC::rePe* embryos where *RC::rePe* is a Cre-responsive GFP reporter at the Rosa26 locus (Ray et al. 2011), permitting isolation of all *Pax3* descendants by fluorescence-activated cell sorting (FACS). Myogenic cells isolated from E13.5 forelimbs or hindlimbs were subsequently cultured and differentiated for 7 d in the presence or absence of Shh protein. Addition of Shh significantly increased the proportion of MyHCI-positive myofibers in the culture (Fig. 2I–J′,M,N). In contrast, the addition of the Smo inhibitor cyclopamine drastically decreased the percentage of slow myofibers when compared with either the vehicle control or cells cultured with Shh protein (Fig. 2K–N). Thus, Shh signaling is capable of inducing slow muscle fiber formation in culture, consistent with our in vivo findings.

Shh signaling is required cell-autonomously for initiation of the myogenic program in the early ventral limb

As Shh signaling has been implicated in regulating *Myf5* expression through Gli2/3 in the somites (Borycki et al. 1999; McDermott et al. 2005), we reasoned that it might similarly promote the myogenic program in a cell-autonomous fashion during limb myogenesis. To study this early aspect of Shh function, we first performed section in situ hybridization to look at the expression of several myogenic differentiation markers between E10.5 and E11.25 in both wild-type and mutant embryos where *Smo* was removed by Pax3^{Cre}. While *Pax3* and *Six1/4* expression was comparable in wild-type and mutant embryos (Fig. 3A,B; Supplemental Fig. 3A–D), cell-autonomous removal of *Smo* resulted in down-regulation of *Myf5* expression at E10.5 in the forelimb ventral muscle mass and at E10.75 in the hindlimb ventral muscle mass (Fig. 3C,D; Supplemental Fig. 4C,D). However, its expression recovered by E10.75 and E11 in the forelimb and hindlimb, respectively, at which point the level of *Myf5* expression became indistinguishable from wild type at the resolution of in situ hybridization. (Fig. 3I,J; Supplemental Fig. 4I,J). Thus, Shh signaling is required for the timely initiation of *Myf5* expression in the early ventral limb muscle but not for ultimately establishing or maintaining its expression. Similar results were obtained by

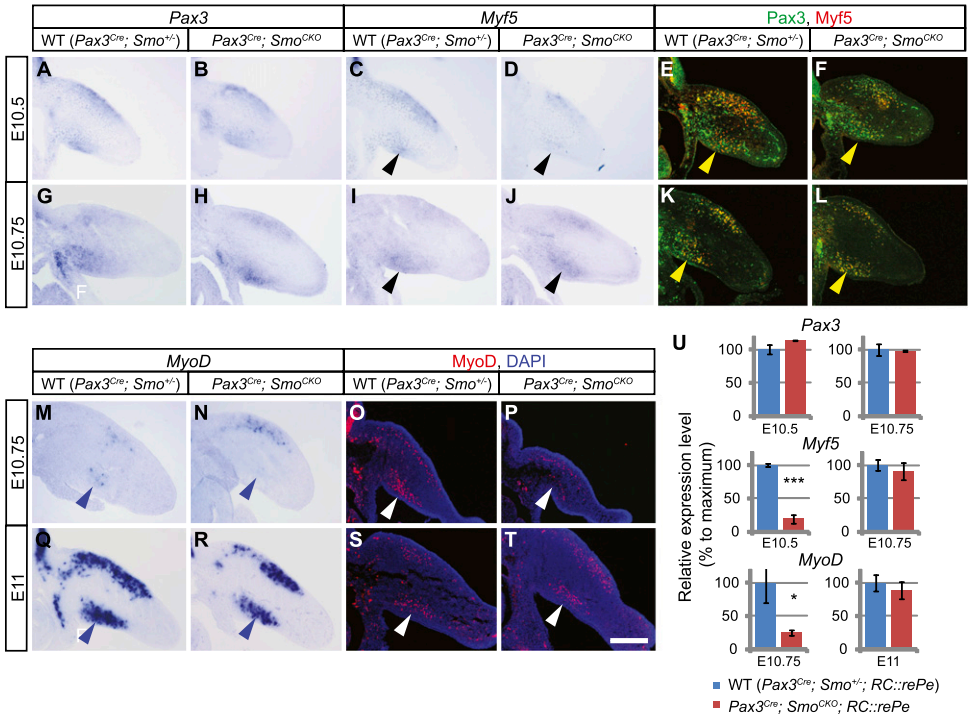

Figure 3. The initiation of the myogenic program is delayed in the *Pax3*^{Cre}*; Smo*^{CKO} mutant forelimb ventral muscle cells. (*A–D*) When Hh signaling is removed cell-autonomously from muscle progenitor cells, section in situ hybridization showed that at E10.5, the initiation of *Myf5* expression was delayed in the *Pax3*^{Cre}*; Smo*^{CKO} mutant forelimb ventral muscle cells (black arrowheads in *C*,*D*). (*A*,*B*) However, *Pax3* expression was unaffected. (*E*,*F*) A similar observation (yellow arrowhead) was made by using antibodies against Myf5 (red) and Pax3 (green). (*G–L*) At E10.75, however, *Myf5* expression had recovered (black and yellow arrowheads). (*M–T*) Like *Myf5*, the initiation of *MyoD* expression was delayed in the *Pax3*^{Cre}*; Smo*^{CKO} mutant forelimb ventral muscle cells at E10.75, as assessed by in situ hybridization (*M*,*N*, blue arrowheads) and immunostaining (*O*,*P*, white arrowheads). (*Q–T*) However, by E11, the expression of both *MyoD* transcripts and MyoD protein was restored. (*U*) A Cre-responsive GFP reporter (*RC::rePe*) was used to generate GFP-positive muscle cells for FACS sorting. Myogenic cells from the ventral forelimb were isolated and analyzed by qPCR, which further demonstrated that the initiation of *Myf5* and *MyoD* expression was delayed in the *Pax3*^{Cre}*; Smo*^{CKO} mutant ventral limb muscle but recovered to almost wild-type levels at a later stage. Expression levels were normalized to *GAPDH* expression. Histograms are expressed as means and standard error of the mean (SEM) ($n = 3$ for each genotype). (***) $P < 0.001$; (*) $P < 0.05$. Bar in *T*: *A–T*, 200 μm.

using Pax3 and Myf5 antibodies (Fig. 3E,F,K,L; Supplemental Fig. 4E,F,K,L).

To further confirm this delay in *Myf5* initiation, we next performed quantitative PCR (qPCR) analysis to quantify *Pax3*, *Six1/4*, and *Myf5* expression in FACS-sorted muscle progenitor cells. GFP-positive myogenic cells were isolated from both *Pax3*^{Cre}*; Smo*^{CKO}*; RC::rePe* mutant and wild-type ventral limbs across different stages. Measurement of RNA expression in these cells confirmed our observation of delayed *Myf5* initiation (Fig. 3U; Supplemental Figs. 3E, S4Q).

This prompted us to further examine *MyoD* expression in order to address whether there was a general delay in the onset of the myogenic differentiation program. Similar to *Myf5*, the onset of *MyoD* expression in the ventral limb muscle was initiated 6 h later in the *Pax3*^{Cre}*; Smo*^{CKO} mutants than in their wild-type counterparts (Fig. 3M–U; Supplemental Fig. 4M–Q), indicating that Shh signaling is required cell-autonomously to promote the early initiation of the myogenic program in the ventral limb. However, as dorsal muscle cell differentiation was largely unaffected and the expression of both *Myf5* and *MyoD* in the ventral muscle mass was ultimately restored, a Shh-independent mechanism must be in place to initiate muscle differentiation in these cells.

Shh signaling is required cell-autonomously for distal limb muscle formation

As noted above, in our analysis of muscle patterning, we observed a loss of muscle in the distal limb bud of *Pax3*^{Cre}*; Smo*^{CKO} mutant limbs (Fig. 4; Supplemental Fig. 5). Indeed, even after *MyoD* expression was restored in the ventral muscle mass at E11, it remained absent in the distal forelimb at E11.5 (Fig. 4A,B). In principle, this could have represented a continuation of the failure in myogenic differentiation in this domain; however, the absence of distal *Pax3* in situ staining at the same developmental stage suggests that the muscle progenitor cells themselves were absent in the mutant autopod (Fig. 4E,F). To confirm this interpretation, we again took advantage of the *RC::rePe* allele to perform recombinase-based fate mapping to definitively establish that no somite-derived cells were present in the distal limb. At

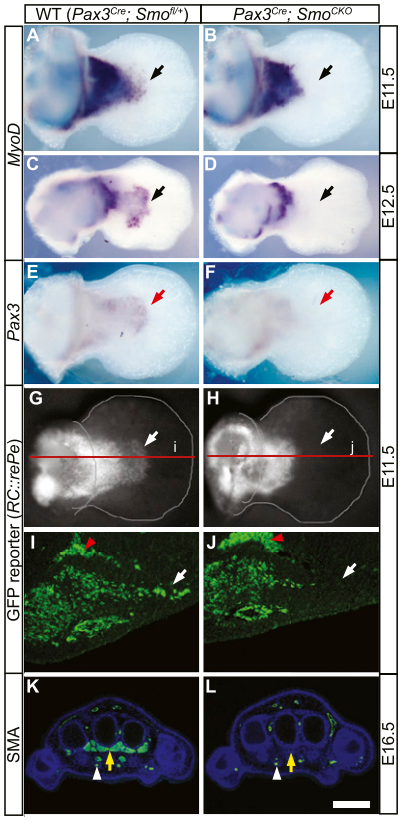

Figure 4. Shh signaling is required cell-autonomously for distal limb muscle formation. (*A*,*C*) The presence of *Myo*D-expressing myogenic cells in the ventral autopod (black arrows) was evident in the wild-type (WT) forelimbs at E11.5 (*A*) and E12.5 (*C*). (*B*,*D*) However, these distal cells were lost in mutant limbs (black arrows), where Hh activity was removed in muscle progenitors. (*E*,*F*) *Pax3* expression was similarly lost in the ventral autopod of $Pax3^{Cre}$; Smo^{CKO} mutants (*F*, red arrow) when compared with the wild-type forelimb (*E*) at E11.5. (*G*–*J*) The loss of distal limb muscles was confirmed by using a Cre-responsive GFP reporter (*RC::rePe*) at E11.5, which marked all *Pax3* descendants, including those in the wild-type distal limb (white arrows in *G*,*I*). (*H*,*J*) However, the autopod *Pax3* descendants was lost in the $Pax3^{Cre}$; Smo^{CKO}; *RC::rePe* mutant limb (white arrows). *I* and *J* are sections through the red lines labeled i and j in *G* and *H*, respectively. Red arrowheads mark autofluorescent blood cells. (*K*,*L*) Using an antibody against SMA, we noted that the early loss of distal myogenic cells led to a complete absence of limb muscles in the $Pax3^{Cre}$; Smo^{CKO} mutant autopod (*L*, yellow arrow) at E16.5, while they were formed normally in the wild-type distal limb (*K*, yellow arrow). Endothelial cells (white arrowheads), also positive for SMA, remain unaffected in the mutant autopod. Bar in *L*: *A*,*B*,*E*–*H*, 320 μm; *C*,*D* 500 μm; *I*,*J*, 80 μm; *K*,*L*, 400 μm.

E11.5, $Pax3^{Cre}$; Smo^{CKO}; *RC::rePe* mutants showed a clear truncation in the distal end of the forelimb ventral muscle mass (Fig. 4G–J). As a consequence of this absence of myogenic cells in the distal limb bud, there is a complete loss of muscles in the forelimb autopod, as indicated by SMA and laminin immunostaining at E16.5 (Fig. 4K,L; Supplemental Fig. 6B′,E′). Similarly, although less affected, the hindlimb autopod exhibited reduced *MyoD* expression at E12.5, which corresponded to a partial muscle loss in the feet at E16.5 (Supplemental Fig. 5A–D).

The loss of distal muscles was also seen in the fate-mapping of descendants of *Pax3*-expressing cells. At E16.5, GFP-positive *Pax3* muscle descendants were present in the stylopod and zeugopod but absent in the autopod of the mutant embryos (Supplemental Fig. 6). Interestingly, GFP-positive endothelial cells that are derived from the somites were unaffected and still present in the autopod blood vessels of *Smo*-deficient animals (Supplemental Fig. 6E). Together, these results indicate that Hh signaling is autonomously required for the formation of distal limb muscles, although dispensable for the more proximal muscle tissues and the vasculature.

Loss of distal limb muscles is not due to increased cell death in the dermomyotome

One potential mechanism that could result in the loss of distal limb muscle is increased cell death in muscle progenitor cells. TUNEL staining and Pax3/anti-cleaved caspase-3 coimmunostaining were performed in order to observe such changes. We found that at E10.25, there was increased apoptosis in the dorsal dermomyotome (data not shown), which could partially explain the dermomyotomal truncation that we observed earlier. At E10.5, cell death also increased at the ventral lateral lip of the dermomyotome, which gives rise to the limb muscles (Fig. 5A–C). However, no increased apoptosis was observed in muscle cells that have migrated into the limb bud, suggesting that Hh signaling is not required for the cell survival once muscle progenitor cells have entered the limb (Fig. 5B; Supplemental Fig. 7B). By E11.5, all abnormal apoptosis was resolved, and the amount of cell death in $Pax3^{Cre}$; Smo^{CKO} was comparable with the wild type (Supplemental Fig. 7A,B).

In order to address whether this initial loss of muscle progenitors in the ventral–lateral dermomyotome could be the cause for the autopod muscle loss, we turned to the chick system, where embryos can be easily manipulated by surgery. We ablated the lateral somites of HH16 or HH20 chick embryos and let them continue to develop in the incubator. The removal of the somites was confirmed by the loss of *Myf5* in situ staining. However, upon further development, the lateral somites eventually grew back, mimicking the recovery of abnormal cell death in E11.5 mouse mutants. Interestingly, no autopod muscle loss was observed (Fig. 5D–G; data not shown). In another experiment, we inserted a metal barrier between the somites and the limb in HH20 chick embryos to delay the entry of muscle cells into the limb bud. Without removal of the barrier, ventral limb muscles failed to form (Supplemental Fig. 7H). However, if the barrier was removed either 24 or 48 h post-insertion, all limb muscles were formed properly (Supplemental Fig. 7I,J), confirming that an initial delay in the entry of the muscle cells into the limb bud does not affect the eventual formation of the distal muscles.

Finally, in an attempt to bypass the initial cell death in mice, we generated $Myf5^{Cre}$; $Smo^{fl/fl}$; and $MyoD^{Cre}$; $Smo^{fl/fl}$ embryos. Both $Myf5^{Cre}$ and $MyoD^{Cre}$ are expressed

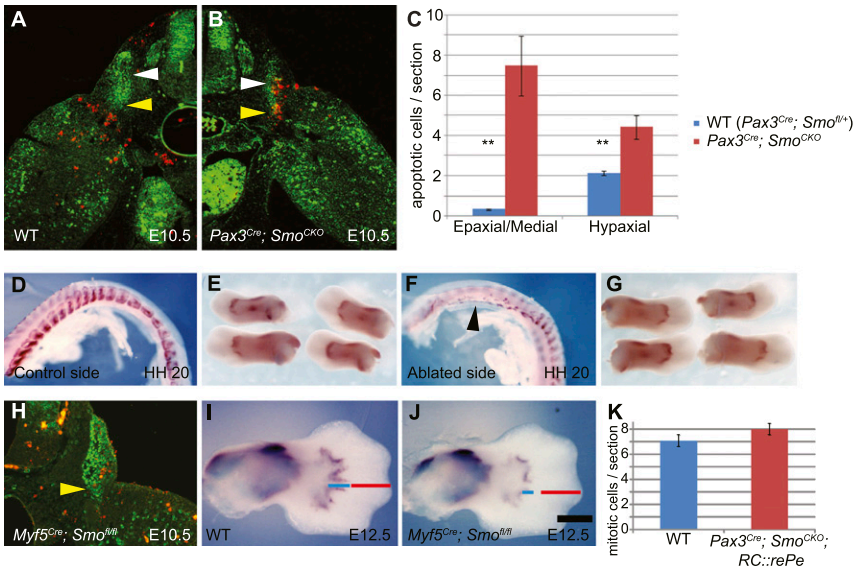

Figure 5. Loss of distal limb muscles is not due to increased cell death in the dermomyotome caused by removal of cell-autonomous Shh activity. (*A*,*B*) Sections of E10.5 wild-type (WT) (*A*) and *Pax3*^{Cre}; *Smo*^{CKO} mutant (*B*) embryos were analyzed for apoptosis, marked by an antibody against cleaved caspase-3 (red), in muscle progenitor cells, labeled by Pax3 antibody (green). Apoptotic cells were counted in the epaxial/medial and hypaxial dermomyotome (white and yellow arrowheads, respectively). (*C*) An increase in apoptosis was observed in both domains of the dermomyotome in the *Pax3*^{Cre}; *Smo*^{CKO} mutants. (*D*–*G*) In the chick system, myogenic cells were marked by *Myf5* in situ hybridization. Early removal of the lateral somite at HH20 (*F*, black arrowhead) did not affect the formation of distal limb muscles in the ventral wing (*G*), which were comparable with the control left side (*D*,*E*). (*H*) In mice, when Hh activity was removed by using Myf5^{Cre}, no apparent apoptosis (marked by red anti-cleave caspase-3 antibody) was observed in the Pax3-labeled (green) hypaxial dermomyotome (yellow arrowhead). (*I*,*J*) However, *MyoD* expression revealed that the distal myocytes in the *Myf5*^{Cre}; *Smo*^{CKO} mutant limb (*J*) did not extend as distally as those in the wild-type limb (*I*) (cf. blue and red lines). (*K*) Finally, the numbers of proliferating myocytes were quantified by using an antibody against phospho-histone-H3 on limb sections from *Pax3*^{Cre}; *Smo*^{CKO}; *RC::rePe* mutants and wild-type siblings at E11.5. No significant difference was detected. Histograms are expressed as means and standard error of the mean (SEM) ($n = 3$ for each genotype). (**) $P < 0.01$. Bar in *J*: *A*,*B*, 300 μm; *D*–*G*, 1 mm; *H*, 200 μm; *I*,*J*, 440 μm.

later than *Pax3*^{Cre} (Chen et al. 2005; Gensch et al. 2008). Removal of *Smo* using either of these Cre drivers results in a normal appearance of the hypaxial dermomyotome, with no evidence of ectopic or increased cell death in the ventral lateral lip (Fig. 5H). In both cases, where Hh signaling was abrogated later than in the *Pax3*^{Cre}; *Smo*^{CKO} mutants, muscles did form to some extent in the autopod but did not extend as distally as the wild-type siblings at E12.5 or E13.5 (Fig. 5I,J; Supplemental Fig. 7E,F), hence giving a milder phenotype that is nonetheless consistent with what we observed in the *Pax3*^{Cre}; *Smo*^{CKO} mutants. Together, these results suggest that it is unlikely that the cell death that we detected in the dermomyotome is the main cause of the distal limb muscle loss in the cell-autonomous mutants.

If increased apoptosis did not play an etiological role in the loss of distal limb muscles, we had to consider the converse explanation that the loss could be due to a decrease in proliferation. This was particularly important to check, as Shh has been shown to act as a mitogen and can affect muscle proliferation in other contexts (Duprez et al. 1998; Bren-Mattison and Olwin 2002). Therefore, we examined muscle cell proliferation in the limb by performing anti-phospho-histone H3 immunostaining at E11. However, no changes in cell proliferation were detected in the limb ventral muscle mass, and it is therefore not likely that a change in proliferation underlies distal muscle loss in the *Pax3*^{Cre}; *Smo*^{CKO} mutants (Fig. 5K).

Hh signaling is required for limb muscle cell migration

Another possible explanation for the loss of distal muscles in the absence of Hh signaling could be that Hh acts cell-autonomously to maintain proper cell migration, allowing muscle progenitor cells to continue their distal migration into the autopod. In order to test whether Hh signaling is required for muscle cell migration, we used in vitro "scratch assays." This assay examines the ability of confluent cells to migrate back into a stripe on a plate, where cells have been removed by creating a scratch. We cultured FACS-sorted GFP- or DsRed-positive myogenic cells that had been harvested from chick embryos following electroporation of pCAG-GFP or -DsRed in the somites. The use of chick embryos allowed us to obtain a large amount of muscle cells, and the inclusion of both GFP and DsRed signals permitted us to easily track cells after imaging. When FACS-sorted primary muscle progenitors were cultured in the presence of Shh protein, they quickly responded to the scratch and migrated over the scratch to close the wound ($n = 3$ of 3) (Fig. 6A; Supplemental Movie 1). However, in the presence of cyclopamine, Hh signaling was inhibited and the cells failed to migrate to the scratched region ($n = 3$ of 3) (Fig. 6A; Supplemental Movie 2). Interestingly, cells that had been treated with cyclopamine did migrate but appeared to be moving randomly, rather than directionally toward the gap. Similar results were obtained using FACS-sorted mouse myogenic cells (Supplemental Movies 3, 4) This therefore suggests a model wherein exposure to Shh is necessary for myoblasts to respond to other directional cues, such as the signals that are generated by cells wounded at the scratch. This raised the possibility that Hh signaling in the limb bud might be similarly required for myogenic cells to respond to directional migratory cues in the distal limb.

To test the plausibility of this model, we examined migrating behavior of myoblasts in vivo. We first analyzed the relative position of the Golgi complex to the nucleus in the muscle progenitor cells from E11 mouse ventral forelimbs, which had a more pronounced distal muscle loss phenotype than the hindlimbs, thereby permitting robust identification of subtle differences. The location of the Golgi apparatus has been found to be at the trailing end of a directionally migrating cell in a three-dimensional (3D) environment and can therefore be used as an indicator of the direction of cell migration (Serrador et al. 1999; Pouthas et al. 2008; Petrie et al. 2009). In GFP-labeled myoblasts within the wild-type limb buds, the Golgi complex was usually found proximal to the nucleus, indicating that muscle progenitors tended to move toward the distal end of the limb bud (Fig. 6B,C). However, the position of the Golgi complex relative to the nucleus was more randomly distributed in the *Pax3^{Cre}; Smo^{CKO}; RC::rePe* mutants, pointing to more randomized cell movements in these embryos (Fig. 6D,E). Thus, in the absence of Shh activity, the migration of limb muscle progenitors becomes less oriented.

Finally, to directly visualize cell migration in vivo, we performed time-lapse imaging on forelimb tissue slices that were prepared from E11 *Pax3^{Cre}; Smo^{CKO}; RC::rePe* mutants and wild-type siblings. In the wild-type limb bud, the GFP-positive muscle cells in the ventral muscle mass were observed to migrate distally over a period of 7.5 h (n = 7 of 9) (Fig. 6F; Supplemental Movie 5). However, such distal movement was rarely detected in *Pax3^{Cre}; Smo^{CKO}; RC::rePe* mutants (n = 10 of 10) (Fig. 6F; Supplemental Movie 6). When cells did initially appear to move distally, they often subsequently wandered back to their original position and made little overall progress toward the distal limb bud (Fig. 6F, yellow arrowheads; Supplemental Movie 4). By tracking individual cells, we were also able to acquire their X and Y coordinates, which were used to calculate the angle of cell turning between each frame. Such analysis revealed that wild-type cells tended to turn distal-ward, in contrast

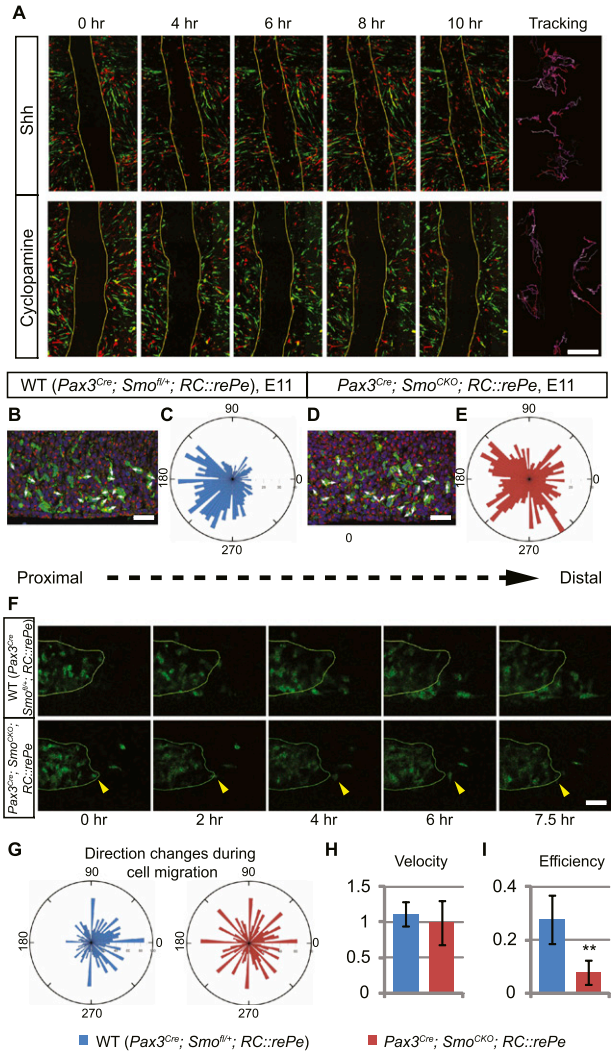

Figure 6. Cell-autonomous Hh activity is required for the migration of distal limb muscle cells. (*A*) Scratch assays were performed to test the requirement of Shh for cell migration. Confluent chick primary muscle cells were labeled with either GFP or DsRed and cultured in the presence of Shh or cyclopamine. Time-lapse images showed that in the presence of Shh, cells began to move into the stripe at the fourth hour and closed the gap by the eighth hour. When Shh signaling was blocked by cyclopamine, cells continued to move but failed to close the gap. Cell movement was tracked, with the beginning of the migration coded white and the subsequent movements coded with increasing red intensity. (*B*,*D*) Sections of E11 mouse ventral limbs (distal to the *right*) were analyzed for the position of the Golgi complex (marked by GM130 antibody, red) relative to the nucleus (DAPI, blue) in *Pax3* descendants (GFP antibody, green). White arrows indicate the directions of cell movements. (*C*,*E*) The relative position of the Golgi to the nucleus was measured as the angle between the Golgi/nucleus alignment and the proximal–distal axis. The numbers of Golgi complexes at a particular angle were quantified and binned at a 5°-interval, as represented on the rosette graph. (*C*) In the wild type (WT), the majority of the Golgi complexes were positioned in the proximal half, indicating distal movements (n = 1157 cells from three individuals). (*E*) In contrast to this, Golgi complexes of muscle progenitor cells that had lost Hh activity were more randomly distributed (n = 1043 cells from three individuals). This difference is statistically significant, with a χ^2 value of 136.312; $P < 0.00001$. (*F*) Time-lapse images of E11 limb tissue slices showed that GFP-positive *Pax3* descendants in the wild-type embryos migrated distally, while *Pax3^{Cre}; Smo^{CKO}; RC::rePe* mutant myogenic cells did not. In a few cases where cells did migrate distally, they often retracted in the end (yellow arrowheads). (*G*) Cells were tracked, and the angle of turning between each frame was quantified, showing that wild-type cells (n = 22) tended to turn toward the distal end of the limb, while mutant cells (n = 19) turn randomly. This difference is statistically significant, with a χ^2 value of 166; $P < 0.00001$. (*H*,*I*) The velocity and efficiency (i.e., ratio between actual displacement and total distance traveled) of these cells were also quantified, showing that while Hh signaling does not affect muscle cell speed, it modulates its migration efficiency. Histograms are expressed as means and standard error of the mean (SEM). (**) $P < 0.01$. Bars: *A*, 500 μm; *B*,*D*, 30 μm; *F*, 40 μm.

to mutant cells, which moved more randomly (Fig. 6G). The velocity and efficiency (directness of the path traversed) of these cells were also calculated, showing that even though both wild-type and mutant cells moved at a comparable speed, wild-type cells were consistently more efficient in reaching their final destination (Fig. 6H,I). Therefore, in agreement with our previous results, Shh activity is required for distally oriented muscle migration.

Net1 acts downstream from Hh signaling to promote continued cell migration

In order to identify potential targets of Hh signaling in the muscle progenitor cells, we FACS-sorted GFP-positive dorsal and ventral muscle cells from E11.25 *Pax3^{Cre}; Smo^{CKO}; RC::rePe* mutant embryos and wild-type *Pax3^{Cre}; Smo$^{fl/+}$; RC::rePe* siblings and extracted RNA for microarray analysis. As expected, both *Smo* itself and the Hh signaling-responsive gene *Ptch1* were down-regulated in the mutants (Table 1). However, we did not detect any change in the expression level of *Pax3* or any of the myogenic regulatory factors (*Myf5*, *MyoD*, and *Myogenin*) at this stage, consistent with our earlier observation that these genes were restored to the wild-type level post-E11.

Interestingly, one of the genes that was significantly down-regulated in *Smo*-deficient myoblasts relative to the wild type was *Net1*. *Net1* encodes a guanine nucleotide exchange factor (GEF) that specifically activates the small GTPase RhoA (Alberts and Treisman 1998). Because RhoA plays an important role during cell migration, it raised the possibility that Hh signaling regulates myogenic cell migration in the limb bud through *Net1*. *Net1* showed a 4.5-fold decrease in the relative expression level in the *Pax3^{Cre}; Smo^{CKO}; RC::rePe* mutant muscles. This down-regulation of *Net1* in muscle cells was validated by whole-mount in situ hybridization in E11 embryo limbs (Fig. 7A–D; Supplemental Fig. 8A–J). Interestingly, its expression appeared to be normal at E10.5, indicating that Hh signaling is not required for *Net1* initiation, in spite of being needed for its maintenance from E10.5 onward.

In order to test the function of *Net1* during muscle migration, we again took advantage of the chick system, where *Net1* is similarly expressed in the limb muscles (data not shown). We electroporated HH18 chick embryo somites at the hindlimb level (somites 26–33) with *GFP* (pCAG-GFP) or two previously described dominant-negative forms of *Net1* (Cag-dnNet1-iresGFP) carrying a deletion in either the Dbl homology (DH) or pleckstrin homology (PH) domain (Guerra et al. 2008). When somitic cells were electroporated with just pCAG-GFP, they continued to migrate and populated the entire muscle mass (n = 7 of 7) (Fig. 7E). However, coelectroporation of both dominant-negative *Net1* constructs severely inhibited muscle migration and even prevented muscle progenitors from entering the limb bud in many cases (n = 18 of 25 affected, nine embryos had no GFP in the limb) (Fig. 7F), demonstrating that *Net1* is indeed required for muscle cell migration.

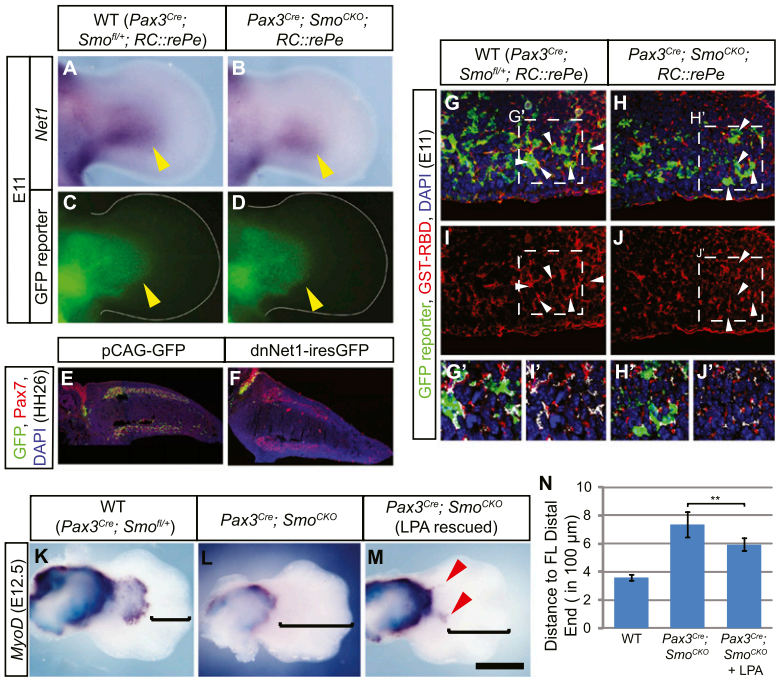

Figure 7. *Net1* acts downstream from Hh signaling to promote cell migration. (*A*,*B*) *Net1* in situ hybridization showed that *Net1* expression was down-regulated in the *Pax3^{Cre}; Smo^{CKO}; RC::rePe* mutant forelimb (*B*, yellow arrowhead) at E11 when compared with the wild-type (WT) limb bud (*A*). (*C*,*D*) This down-regulation was not due to a loss of muscle progenitors in the limb, marked by the Pax3^{Cre}-responsive GFP reporter. (*E*,*F*) In the chick system, when the lateral somites at the hindlimb level were electroporated with pCAG-GFP at HH18, GFP-positive cells (green) were found throughout the *Pax*7-positive dorsal and ventral muscle masses (red) at HH26 (shown in *E*). (*F*) However, when two dominant-negative forms of *Net1* were coelectroporated into the lateral somites, cells failed to migrate into the limb, demonstrating that functional Net1 activity is required for muscle cell migration. (*G–J*) Active RhoA, as detected by GST-RBD, was reduced in the *Pax3^{Cre}; Smo^{CKO}; RC::rePe* mutant forelimb ventral muscle cells, marked by the Cre-responsive GFP reporter, at E11 (white arrowheads). (*G′–J′*) Blow-ups of the squares in *G–J* show that there are less overlapping green and red signals (white patches) in the mutant myogenic cells. (*K–M*) The loss of distal forelimb muscles in the *Pax3^{Cre}; Smo^{CKO}* mutants was partially rescued (red arrowheads) by serial injection of the RhoA activator LPA. (*N*) This rescue can be quantified as the distance from the distal-most *MyoD* staining to the tip of the hand plate (as indicated by the brackets in *K–M*). Histograms are expressed as means and standard error of the mean (SEM) (n = 6 for each genotype). (**) $P < 0.01$. Bar in *M*: *A–D*, 315 μm; *E*,*F*, 350 μm; *G–J*, 60 μm; *G′–J′*, 45 μm; *K–M*, 500 μm.

These results are consistent with the view that, in the normal limb bud, Hh signaling is required to maintain *Net1* expression in the migrating myoblasts. In the absence of Hh signaling, *Net1* is down-regulated, which could be predicted to render reduced RhoA activity. Indeed, by using GST-RBD to label active RhoA and an antibody to detect GST, it became apparent that in the mutant ventral limb, there was diminished RhoA activity in the distal muscle cells (Fig. 7G–J′), which likely led to inefficient cell migration at E11 and the loss of distal muscles at E11.5. This model would therefore suggest that it might be possible to rescue the *Smo*-deficient phenotype by restoring RhoA activity. We injected lysophosphotidic acid (LPA), a RhoA activator, into pregnant female mice starting at E9.5 and every 0.5 d afterward until E11.5. This treatment was able to partially rescue the loss of distal muscle in $Pax3^{Cre}$; Smo^{CKO} mutants at E12.5 (n = 5 of 6) (Fig. 7K–N; Supplemental Fig. 9). While the rescue was incomplete, we also noted that *Dock9*, a GEF for another small GTPase, CDC42, was additionally down-regulated in the $Pax3^{Cre}$; Smo^{CKO} mutants (Table 1; Supplemental Fig. 8K–N), hinting at a common theme of migratory regulation by the Hh signaling.

Discussion

By conditionally removing Smo activity, and hence the ability to respond to Hh signaling, from various cell populations in the limb, we demonstrated that the function of Hh during limb muscle development is multifaceted and that Hh signaling acts both cell-autonomously and non-cell-autonomously in directing limb muscle formation. A parallel study by Anderson et al. (2012) also reached similar conclusions.

We observed that when Hh signaling is disrupted in the lateral plate-derived limb mesenchyme, normal muscle AP patterning is lost and the resultant muscle bundles are more symmetrical. The nonmuscle mesenchyme has long been considered as the main source for muscle patterning, and it has been established that the muscle connective tissue sets up a prepattern for correct muscle patterning to take place (Christ et al. 1977; Jacob and Christ 1980; Kardon et al. 2003; Hasson et al. 2010). Our results further confirm this notion and show that Shh does not pattern limb muscles directly but through the lateral plate-derived cells.

Hh signaling also promotes slow muscle fiber myogenesis in a cell-autonomous fashion. This finding is consistent with a previous study demonstrating that muscle cells are responsive to Hh signaling after they have migrated into the limb between E10.5 and E11.5 (Ahn and Joyner 2004). Whether these cells are responding to Shh or Ihh remains unclear. While Ihh from the developing long bones could be responsible for this, we cannot rule out the possibility that at an earlier stage, Shh sets up cellular memory of exposure in a population of muscle cells that are destined to form the slow fibers. When fiber type becomes specified in myogenic cells has been controversial. For example, at least in birds, it has been shown that the first muscle progenitor cells to enter the limb contribute to the proximal slow muscles and that the fast muscles are formed by later-migrating populations (Van Swearingen and Lance-Jones 1995). However, other studies have suggested that cell fate is not predetermined in the somites (Kardon et al. 2002; Rees et al. 2003).

Regardless of the timing of slow muscle determination, the cell-autonomous requirement for Hh signaling that we observed in our study is similar to that seen in the formation of zebrafish adaxial slow muscle fibers (Baxendale et al. 2004; Feng et al. 2006). However, contrary to the near complete loss of slow fibers in zebrafish *smo* mutants (Barresi et al. 2000), there is only ~20% reduction in the $Pax3^{Cre}$; Smo^{CKO} mutants, suggesting that additional mechanisms are in place for specifying the slow fiber myogenesis in the mammalian limbs. Additional regulation of this process is likely provided by the muscle connective tissue, which is known to affect slow fiber myogenesis via the WNT/β-catenin pathway (Anakwe et al. 2003; Mathew et al. 2011).

We did not see any significant changes in proliferation of the limb myogenic cells in the absence of cell-autonomous Hh signaling. We also did not see any increase in myogenic cell death within the limb bud. Similar results were obtained in the parallel study by Anderson et al. (2012). However, we did detect cell death in both the epaxial and hypaxial dermomyotome in the $Pax3^{Cre}$; Smo^{CKO} mutants. Our finding that dermomyotomal cell survival depends on cell-autonomous Hh signaling is intriguing as, while Shh has been shown to be critical for cell survival in the ventral somite, it is considered to be dispensable for the developing dermomyotome (Borycki et al. 1999). This discrepancy could be due to the stage and the somite level of the embryo at the time of apoptosis detection, as apoptosis occurs transiently at E10.5 and is more apparent in the more mature somites at the forelimb level than in those at the hindlimb level. It is also possible that *Ihh* from the endoderm maintains the survival of dermomyotomal cells in the previously analyzed *Shh* mutants, while the removal of *Smo* alleles in our study blocks all Hh activity. Indeed, at least at E8.5, the Hh response gene *Ptch1* is still expressed in the somites of *Shh*-null embryos. Moreover, in general, *Smo* mutants phenocopy $Shh^{-/-}$; $Ihh^{-/-}$ double mutants, which have more severe phenotypes than the $Shh^{-/-}$ single mutant (Zhang et al. 2001).

The Hh signaling pathway in the limb has been previously shown to drive myogenic proliferation (Duprez et al. 1998), maintain cell survival (Kruger et al. 2001), and regulate the size of the muscle progenitor pool in the limb (and hence muscle mass within the limb) by controlling myoblast proliferation and differentiation during primary myogenesis and maintaining cell survival over secondary myogenesis (Bren-Mattison and Olwin 2002; Bren-Mattison et al. 2011). However, it was unclear whether these processes were direct effects of cell-autonomous Shh function. By removing *Smo* specifically from muscle progenitor cells, both this work and that of the accompanying study by Anderson et al. (2012) demonstrated a cell-autonomous requirement for Shh to initiate the myogenic program in the early ventral muscle mass. In this context, Shh

appears to function similar to its role in the somites to directly regulate the expression of *Myf5* (Borycki et al. 1999; McDermott et al. 2005). However, as the expression of *Myf5* and *MyoD* in the ventral muscle cells recovered and the dorsal muscle mass was largely unaffected, additional mechanisms must be in place to compensate for the loss of Shh signaling in order to initiate the myogenic differentiation program. Moreover, as noted above, neither cell proliferation nor survival was affected in the absence of cell-autonomous Shh activity; these effects of loss of Shh observed in previous studies are therefore most likely due to non-cell-autonomous Shh function mediated by other tissue types.

Both our work and that of Anderson et al. (2012) further identified a specific loss of distal muscles when Shh responsiveness was conditionally removed from the myogenic cells. This could be the result of the loss of early *Myf5* and *MyoD* expression. In this scenario, proper Shh-induced myogenic differentiation may be required at the beginning of limb myogenesis to specify a subpopulation that will eventually become the distal limb muscle. However, our study strongly suggests that there is also a cell-autonomous requirement for Hh signaling to maintain proper muscle cell migration within the limb. These explanations are certainly not mutually exclusive, and it is additionally plausible that a prompt onset of myogenic differentiation is required to maintain *Net1* expression for Hh-dependent muscle migration.

Shh has previously been reported to regulate cell movement in various contexts, such as medial migration of the endothelial progenitors in zebrafish, the navigation of axons in the neural tube, the distribution of oligodendrocytes along the developing optic nerves, and the migration of adult neural precursor cells to the olfactory bulb (Charron et al. 2003; Gering and Patient 2005; Merchán et al. 2007; Angot et al. 2008; Yam et al. 2009). In these cases, however, Shh acts as a chemoattractant, which is unlikely to be the governing mechanism by which Hh signaling regulates limb muscle migration because *Shh* is expressed in the posterior limb bud and muscle cells migrate distally.

In cell culture studies, Shh has been shown to be required for cell motility by activating Rho GTPases through a "non-canonical" or Gli-independent pathway (Renault et al. 2010; Sasaki et al. 2010; Polizio et al. 2011). In these scenarios, signaling activation is relayed from Smo to the G proteins or Tiam1, a GEF for Rac1 (Sasaki et al. 2010; Polizio et al. 2011). While we cannot rule out these possibilities, our results strongly indicate that in the limb myogenic cells, Hh signaling is required cell-autonomously to maintain the expression of *Net1*, which is in turn required for adequate RhoA activity and cell migration.

From our study, a model for the regulation of limb muscle development by the Hh signaling pathway emerges (Fig. 8). As limb muscle progenitor cells are formed at the ventral lateral lip of the dermomyotome, Shh from the midline is transiently required cell-autonomously at E10.5 to promote their survival. Subsequently, Shh from the ZPA patterns the lateral plate-derived limb mesenchyme along the AP axis, which in turn patterns the

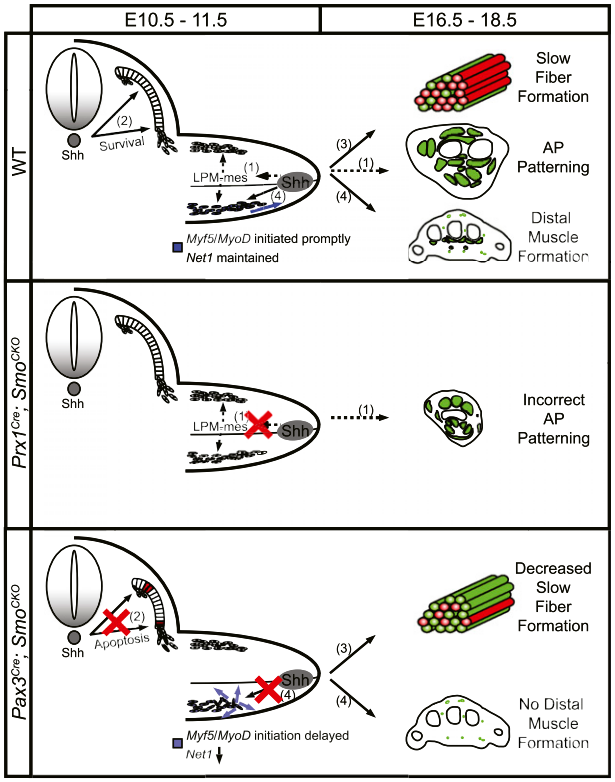

Figure 8. Schematic representation of the function of Shh during limb muscle development. In normal conditions, Shh patterns limb muscles non-cell-autonomously along the AP axis through the lateral plate-derived limb mesenchyme (1) such that when Hh activity is removed in the nonmuscle limb mesenchyme by Prx1-Cre recombinase AP patterning of the limb muscles is affected. Meanwhile, cell-autonomous function of Hh signaling is required to maintain cell survival in the dermomyotome (2), promote the formation of slow muscle fibers (3), initiate *Myf5* and *MyoD* expression in a timely manner, and regulate directional migration of the distal myocytes by maintaining *Net1* expression (4). Thus, in the absence of Hh activity in the muscle progenitor cells, there is increased apoptosis in the dermomyotome, decreased slow muscle fibers, and loss of distal muscles.

muscle progenitor cells that have migrated into the limb bud. At the same time, Shh promotes the early phase of myogenic differentiation and maintains *Net1* expression cell-autonomously in the migrating muscle cells. Net1 is the GEF for RhoA, and its up-regulation by Shh signaling is permissively required for continued muscle cell migration toward the distal limb bud between E10.5 and E11.5. Consequently, in the absence of Shh signaling in the muscle progenitor cells, *Net1* is down-regulated, and directionally persistent migration is lost in these cells, resulting in the truncation of distal muscles. At a later stage, myocytes undergo terminal differentiation, and again Hh signaling is required cell-autonomously to promote slow muscle fiber formation, which is key to establishing optimally functional adult muscles.

Last, the vertebrate limb has been thought to have evolved in two phases: The proximal structures are Shh-

independent and more basal, and the distal structures are Shh-dependent and evolutionarily novel (Shubin and Alberch 1986; Ahlberg and Milner 1994; Sordino et al. 1995; Kardon 1998; Francis-West et al. 2003). In addition, while *Shh* expression persists until the beginning of digit formation in the tetrapods, it disappears at an earlier stage, prior to ray formation in the teleosts, which lack muscles in the fin ray region (López-Martínez et al. 1995; Sordino et al. 1995; Thorsen and Hale 2005). Therefore, despite the ongoing debate on the evolutionary origin of the autopod in the tetrapods (Holmgren 1933; Gregory and Raven 1941; Wagner and Chiu 2001; Shubin et al. 2006; Boisvert et al. 2008), it is tempting to propose that early tetrapods have co-opted an existing pathway (Shh signaling from ZPA) to extend the distribution of the limb muscles to the more distally located and structurally complicated autopod, a potentially neomorphic structure.

Materials and methods

Mouse genetics and manipulations

$Smo^{fl/fl}$, $Smo^{del/+}$, $Pax3^{Cre}$, $Prx1^{Cre}$, $Myf5^{Cre}$, $MyoD^{Cre}$, and $Tcf4^{GFPCre+neo}$ mice and *RC::rePe* (Cre-responsive GFP reporter) were previously reported and genotyped as described (Long et al. 2001; Logan et al. 2002; Chen et al. 2005; Engleka et al. 2005; Gensch et al. 2008; Purcell et al. 2009; Mathew et al. 2011; Ray et al. 2011). Generation of mutant embryos and wild-type siblings are described in the text. Noon of the day of vaginal plug discovery was designated as E0.5. For the microarray analysis of gene expression level, dissociated ventral and dorsal E11.25 limb mesenchyme was FACS-sorted (Hematologic Neoplasia Flow Cytometry Facility at Dana-Farber Cancer Institute), and RNA was extracted using the RNeasy kit (Qiagen). Fifty-eight $Pax3^{Cre}$; Smo^{CKO}; *RC::rePe* mutant forelimbs and 55 wild-type sibling forelimbs were pooled into three different samples for triplicate. Microarray was performed on the Illumina Mouse WG-6 Expression BeadChip by the Molecular Genetics Core Facility at Children's Hospital Boston (supported by NIH-P50-NS40828 and NIH-P30-HD18655). For qPCR analysis, RNA from FACS-sorted muscle cells at different stages (as indicated in the text) was reverse-transcribed to cDNA using SuperScript VILO cDNA Synthesis kit (Invitrogen). qPCR was performed using the Roche LightCycler with the following conditions: 2 min at 95°C and 40 cycles of amplification (5 sec at 95°C, 10 sec at 56°C, and 20 sec at 72°C). The primer sets used are listed in Supplemental Table 1. All measurements were normalized to *GAPDH* and *β-actin*. A water sample was used as the negative control and set as 0% for expression level. An in vitro differentiation assay was performed as previously described (Mathew et al. 2011). Rescue of the distal muscle loss in the Smo^{CKO}; $Pax3^{Cre}$ mutant limbs was done by intraperitoneal injection of LPA (20 μg/g body weight) at E9.5. Serial injections were subsequently made every 12 h until E11.5.

Chick embryos, surgeries, and electroporation

Fertilized chick eggs from commercial sources (Charles River) were incubated at 38°C and staged according to Hamburger and Hamilton (1951). Lateral somite ablation was done by cutting the lateral 200 μm of somite 16–21 using a sharpened tungsten needle. The barrier experiment was performed by inserting a tantalum foil barrier between the developing limb bud and the somites at HH20. The barriers were either left in situ or removed 24 or 48 h after insertion. Embryos were either immediately processed for whole-mount in situ hybridization to check *Myf5* expression in the somites or put back into the incubator to allow further development until HH26 or HH34 to assess limb muscle formation. Somite electroporation experiments were carried out as previously described (Scaal et al. 2004). pCAG-GFP was used as a positive control (Matsuda and Cepko 2004). Dominant-negative *Net1* alleles carrying a deletion in the DH or PH domain were gifts from Alan Hall (Memorial Sloan-Kettering Cancer Center) and were subcloned into pCAGIG (Matsuda and Cepko 2004).

In situ hybridization and immunohistochemistry

For whole-mount in situ hybridization, samples were fixed in 4% PFA overnight at 4°C, and the hybridization was carried out as previously described (Riddle et al. 1993). DIG-labeled probes were detected with NBT/BCIP (Sigma) or BM Purple (Roche). Probes include mouse *MyoD* (Brent et al. 2003), mouse *Pax3* (Goulding et al. 1991), chick *Myf5* (Brent and Tabin 2004), mouse *Net1* (RT–PCR product using primers 5′-TGGGAGCATCAAG GGTTACT-3′ and 5′-AATGAATGCAGAAGGCGAAC-3′), and mouse *Dock9* (RT–PCR product using primers 5′-GGGA CATGCTTTGTCATGTG-3′ and 5′-TCAGTGCTGCTTTGTC TGCT-3′). For antibody staining, all samples were fixed in 4% PFA for 4–6 h at 4°C (unless stated otherwise in Supplemental Table 2) and prepared for either frozen or paraffin sectioning. The primary antibodies used are tabulated in Supplemental Table 2. Secondary antibodies (Molecular Probes) used include Alexa Fluor 594 goat anti-rabbit IgG, Alexa Fluor 488 goat anti-rabbit IgG, Alexa Fluor 594 goat anti-mouse IgG, and Alexa Fluor 488 goat anti-chick IgG (all at 1:250 dilution for 1 h at room temperature). For active RhoA detection, sectioned samples were blocked in 0.05% BSA in HBS before GST-RBD (Cytoskeleton) application. GST-RBD was diluted in HBS at a concentration of 200 μg/mL and incubated with samples for 90 min at room temperature. Samples were fixed for 15 sec with cold acetone–formalin before antibody detection.

Scratch assay

Chick somites at the hindlimb level were electroporated with pCAG-GFP or pCAG-DsRed (Matsuda and Cepko 2004) at HH18 and allowed to develop at 38°C until HH25/26. In experiments where Hh signaling was to be abrogated, 1 μg of cyclopamine (Calbiochem) was delivered to the electroporated chick embryos by pipetting. Cyclopamine was prepared as previously described (Incardona et al. 1998). HH25/26 limb mesenchyme was subsequently incubated in 0.5% trypsin for 10 min at room temperature and dissociated by pipetting in DMEM/10% FBS. Dissociated cells were FACS-sorted for GFP- or DsRed-positive myogenic cells, which were then plated in a 96-well plate with a glass bottom (MatTek) coated with ECL (entactin-collagen IV-laminin; Millipore). The plated cells were incubated in DMEM/20% FBS/2.5 ng/mL bFGF plus either 20 nM Shh protein (Curis) or 50 μM cyclopamine for 24 h at 37°C with 5% CO_2 to reach confluence, and a scratch wound was generated by a fine pipette tip. Cell migration was recorded by performing time-lapse microscopy.

Time-lapse microscopy and image analysis

Time-lapse imaging was performed as previously described (Gros et al. 2010). Myogenic cells at the scratch wound were imaged every 8 min for 12 h at 37°C and 5% CO_2 at a wavelength of 910 nm to capture the migration of both GFP- and DsRed-positive

myogenic cells. For live imaging of limb explants, E10.75–E11 mouse embryos were dissected in PBS and sectioned manually at a thickness of ~200 μm using obsidian scalpels (Fine Science Tools). The tissue slices were cultured in 40% DMEM/60% rat serum (Harlan Laboratories)/1% low-melting agarose/0.5% glucose/2.5 mM HEPES (Gibco)/1% penicillin–streptomycin, supplemented with 20 nM of Shh protein (Curis). Images of ventral limb muscle mass were taken at 850 nm every 5 min for 12 h. Time-lapse movies were generated using NIH ImageJ, and cells were tracked using the manual tracking plug-in contributed by Fabrice Cordeli. Colocalization of active RhoA signals and muscle cells was done by using the ImageJ colocalization plug-in contributed by Pierre Bourdoncle.

Acknowledgments

We thank Jérôme Gros for technical advice with confocal live imaging and electroporation. We also thank Susan Dymecki, Jonathon Epstein, Gabrielle Kardon, and Andrew McMahon for mouse strains. B.D.H. was funded by the March of Dimes. This work was supported by NIH/NICHD grant R37HD032443 to C.J.T.

References

Agbulut O, Noirez P, Beaumont F, Butler-Browne G. 2003. Myosin heavy chain isoforms in postnatal muscle development of mice. *Biol Cell* **95:** 399–406.

Ahlberg PE, Milner AR. 1994. The origin and early diversification of tetrapods. *Nature* **368:** 507–514.

Ahn S, Joyner AL. 2004. Dynamic changes in the response of cells to positive hedgehog signaling during mouse limb patterning. *Cell* **118:** 505–516.

Alberts AS, Treisman R. 1998. Activation of RhoA and SAPK/JNK signalling pathways by the RhoA-specific exchange factor mNET1. *EMBO J* **17:** 4075–4085.

Alcedo J, Ayzenzon M, Von Ohlen T, Noll M, Hooper JE. 1996. The *Drosophila* smoothened gene encodes a seven-pass membrane protein, a putative receptor for the hedgehog signal. *Cell* **86:** 221–232.

Anakwe K, Robson L, Hadley J, Buxton P, Church V, Allen S, Hartmann C, Harfe B, Nohno T, Brown AMC, et al. 2003. Wnt signalling regulates myogenic differentiation in the developing avian wing. *Development* **130:** 3503–3514.

Anderson C, Williams VC, Moyon B, Daubas P, Tajbakhsh S, Buckingham ME, Shiroishi T, Hughes SM, Borycki A-G. Sonic hedgehog acts cell-autonomously on muscle precursor cells to generate limb muscle diversity. (this issue). doi: 10.1101/gad.187807.112.

Angot E, Loulier K, Nguyen-Ba-Charvet KT, Gadeau A-P, Ruat M, Traiffort E. 2008. Chemoattractive activity of sonic hedgehog in the adult subventricular zone modulates the number of neural precursors reaching the olfactory bulb. *Stem Cells* **26:** 2311–2320.

Barresi MJ, Stickney HL, Devoto SH. 2000. The zebrafish slow-muscle-omitted gene product is required for Hedgehog signal transduction and the development of slow muscle identity. *Development* **127:** 2189–2199.

Baxendale S, Davison C, Muxworthy C, Wolff C, Ingham Philip W, Roy S. 2004. The B-cell maturation factor Blimp-1 specifies vertebrate slow-twitch muscle fiber identity in response to Hedgehog signaling. *Nat Genet* **36:** 88–93.

Birchmeier C, Brohmann H. 2000. Genes that control the development of migrating muscle precursor cells. *Curr Opin Cell Biol* **12:** 725–730.

Boisvert CA, Mark-Kurik E, Ahlberg PE. 2008. The pectoral fin of *Panderichthys* and the origin of digits. *Nature* **456:** 636–638.

Borycki AG, Brunk B, Tajbakhsh S, Buckingham M, Chiang C, Emerson CP Jr. 1999. Sonic hedgehog controls epaxial muscle determination through Myf5 activation. *Development* **126:** 4053–4063.

Bouldin CM, Gritli-Linde A, Ahn S, Harfe BD. 2010. Shh pathway activation is present and required within the vertebrate limb bud apical ectodermal ridge for normal autopod patterning. *Proc Natl Acad Sci* **107:** 5489–5494.

Bren-Mattison Y, Olwin BB. 2002. Sonic hedgehog inhibits the terminal differentiation of limb myoblasts committed to the slow muscle lineage. *Dev Biol* **242:** 130–148.

Bren-Mattison Y, Hausburg M, Olwin BB. 2011. Growth of limb muscle is dependent on skeletal-derived Indian hedgehog. *Dev Biol* **356:** 486–495.

Brent AE, Tabin CJ. 2004. FGF acts directly on the somitic tendon progenitors through the Ets transcription factors Pea3 and Erm to regulate scleraxis expression. *Development* **131:** 3885–3896.

Brent AE, Schweitzer R, Tabin CJ. 2003. A somitic compartment of tendon progenitors. *Cell* **113:** 235–248.

Bryson-Richardson RJ, Currie PD. 2008. The genetics of vertebrate myogenesis. *Nat Rev Genet* **9:** 632–646.

Cann GM, Lee JW, Stockdale FE. 1999. Sonic hedgehog enhances somite cell viability and formation of primary slow muscle fibers in avian segmented mesoderm. *Anat Embryol* **200:** 239–252.

Charron F, Stein E, Jeong J, McMahon AP, Tessier-Lavigne M. 2003. The morphogen sonic hedgehog is an axonal chemoattractant that collaborates with netrin-1 in midline axon guidance. *Cell* **113:** 11–23.

Chen JCJ, Mortimer J, Marley J, Goldhamer DJ. 2005. MyoD-cre transgenic mice: A model for conditional mutagenesis and lineage tracing of skeletal muscle. *Genesis* **41:** 116–121.

Chevallier A, Kieny M, Mauger A. 1977. Limb–somite relationship: Origin of the limb musculature. *J Embryol Exp Morphol* **41:** 245–258.

Chiang C, Litingtung Y, Harris MP, Simandl BK, Li Y, Beachy PA, Fallon JF. 2001. Manifestation of the limb prepattern: Limb development in the absence of sonic hedgehog function. *Dev Biol* **236:** 421–435.

Christ B, Jacob HJ, Jacob M. 1977. Experimental analysis of the origin of the wing musculature in avian embryos. *Anat Embryol (Berl)* **150:** 171–186.

Dhouailly D, Kieny M. 1972. The capacity of the flank somatic mesoderm of early bird embryos to participate in limb development. *Dev Biol* **28:** 162–175.

Duprez D, Fournier-Thibault C, Le Douarin N. 1998. Sonic Hedgehog induces proliferation of committed skeletal muscle cells in the chick limb. *Development* **125:** 495–505.

Duprez D, Lapointe F, Edom-Vovard F, Kostakopoulou K, Robson L. 1999. Sonic hedgehog (SHH) specifies muscle pattern at tissue and cellular chick level, in the chick limb bud. *Mech Dev* **82:** 151–163.

Echelard Y, Epstein DJ, St-Jacques B, Shen L, Mohler J, McMahon JA, McMahon AP. 1993. Sonic hedgehog, a member of a family of putative signaling molecules, is implicated in the regulation of CNS polarity. *Cell* **75:** 1417–1430.

Engleka KA, Gitler AD, Zhang M, Zhou DD, High FA, Epstein JA. 2005. Insertion of Cre into the Pax3 locus creates a new allele of Splotch and identifies unexpected Pax3 derivatives. *Dev Biol* **280:** 396–406.

Feng X, Adiarte EG, Devoto SH. 2006. Hedgehog acts directly on the zebrafish dermomyotome to promote myogenic differentiation. *Dev Biol* **300:** 736–746.

Francis-West PH, Antoni L, Anakwe K. 2003. Regulation of myogenic differentiation in the developing limb bud. *J Anat* **202:** 69–81.

Gensch N, Borchardt T, Schneider A, Riethmacher D, Braun T. 2008. Different autonomous myogenic cell populations revealed by ablation of Myf5-expressing cells during mouse embryogenesis. *Development* **135:** 1597–1604.

Gering M, Patient R. 2005. Hedgehog signaling is required for adult blood stem cell formation in zebrafish embryos. *Dev Cell* **8:** 389–400.

Goulding MD, Chalepakis G, Deutsch U, Erselius JR, Gruss P. 1991. Pax-3, a novel murine DNA binding protein expressed during early neurogenesis. *EMBO J* **10:** 1135–1147.

Gregory WK, Raven HC. 1941. Studies on the origin and early evolution of paired fins and limbs. *Ann N Y Acad Sci* **42:** 273–360.

Gros J, Hu JH, Vinegoni C, Feruglio PF, Weissleder R, Tabin CJ. 2010. WNT5A/JNK and FGF/MAPK pathways regulate the cellular events shaping the vertebrate limb bud. *Curr Biol* **20:** 1993–2002.

Guerra L, Carr HS, Richter-Dahlfors A, Masucci MG, Thelestam M, Frost JA, Frisan T. 2008. A bacterial cytotoxin identifies the RhoA exchange factor Net1 as a key effector in the response to DNA damage. *PLoS ONE* **3:** e2254. doi: 10.1371/journal.pone.0002254.

Gunning P, Hardeman E. 1991. Multiple mechanisms regulate muscle fiber diversity. *FASEB J* **5:** 3064–3070.

Gustafsson MK, Pan H, Pinney DF, Liu Y, Lewandowski A, Epstein Douglas J, Emerson CP Jr. 2002. Myf5 is a direct target of long-range Shh signaling and Gli regulation for muscle specification. *Genes Dev* **16:** 114–126.

Hamburger H, Hamilton V. 1951. A series of normal stages in the development of the chick embryo. *J Morphol* **88:** 49–92.

Hasson P, DeLaurier A, Bennett M, Grigorieva E, Naiche LA, Papaioannou VE, Mohun TJ, Logan MPO. 2010. Tbx4 and tbx5 acting in connective tissue are required for limb muscle and tendon patterning. *Dev Cell* **18:** 148–156.

Holmgren N. 1933. On the origin of the tetrapod limb. *Acta Zoologica* **14:** 185–295.

Huang R, Zhi Q, Christ B. 2003. The relationship between limb muscle and endothelial cells migrating from single somite. *Anat Embryol (Berl)* **206:** 283–289.

Hutcheson DA, Zhao J, Merrell A, Haldar M, Kardon G. 2009. Embryonic and fetal limb myogenic cells are derived from developmentally distinct progenitors and have different requirements for β-catenin. *Genes Dev* **23:** 997–1013.

Incardona JP, Gaffield W, Kapur RP, Roelink H. 1998. The teratogenic *Veratrum* alkaloid cyclopamine inhibits sonic hedgehog signal transduction. *Development* **125:** 3553–3562.

Jacob HJ, Christ B. 1980. On the formation of muscular pattern in the chick limb. In *Teratology of the limbs* (ed. HJ Merker et al.), pp. 89–97. Walter de Gruyter and Co., Berlin.

Kardon G. 1998. Muscle and tendon morphogenesis in the avian hind limb. *Development* **125:** 4019–4032.

Kardon G, Campbell JK, Tabin CJ. 2002. Local extrinsic signals determine muscle and endothelial cell fate and patterning in the vertebrate limb. *Dev Cell* **3:** 533–545.

Kardon G, Harfe BD, Tabin CJ. 2003. A Tcf4-positive mesodermal population provides a prepattern for vertebrate limb muscle patterning. *Dev Cell* **5:** 937–944.

Kruger M, Mennerich D, Fees S, Schafer R, Mundlos S, Braun T. 2001. Sonic hedgehog is a survival factor for hypaxial muscles during mouse development. *Development* **128:** 743–752.

Li X, Blagden CS, Bildsoe H, Bonnin MA, Duprez D, Hughes SM. 2004. Hedgehog can drive terminal differentiation of amniote slow skeletal muscle. *BMC Dev Biol* **4:** 9. doi: 10.1186/1471-213X-4-9.

Li Y, Qiu Q, Watson SS, Schweitzer R, Johnson RL. 2010. Uncoupling skeletal and connective tissue patterning: Conditional deletion in cartilage progenitors reveals cell-autonomous requirements for Lmx1b in dorsal-ventral limb patterning. *Development* **137:** 1181–1188.

Logan M, Martin JF, Nagy A, Lobe C, Olson EN, Tabin CJ. 2002. Expression of Cre Recombinase in the developing mouse limb bud driven by a Prxl enhancer. *Genesis* **33:** 77–80.

Long F, Zhang XM, Karp S, Yang Y, McMahon AP. 2001. Genetic manipulation of hedgehog signaling in the endochondral skeleton reveals a direct role in the regulation of chondrocyte proliferation. *Development* **128:** 5099–5108.

López-Martínez A, Chang DT, Chiang C, Porter JA, Ros MA, Simandl BK, Beachy PA, Fallon JF. 1995. Limb-patterning activity and restricted posterior localization of the amino-terminal product of Sonic hedgehog cleavage. *Curr Biol* **5:** 791–796.

Mathew SJ, Hansen JM, Merrell AJ, Murphy MM, Lawson JA, Hutcheson DA, Hansen MS, Angus-Hill M, Kardon G. 2011. Connective tissue fibroblasts and Tcf4 regulate myogenesis. *Development* **138:** 371–384.

Matsuda T, Cepko CL. 2004. Electroporation and RNA interference in the rodent retina in vivo and in vitro. *Proc Natl Acad Sci* **101:** 16–22.

McDermott A, Gustafsson M, Elsam T, Hui C-C, Emerson CP Jr, Borycki A-G. 2005. Gli2 and Gli3 have redundant and context-dependent function in skeletal muscle formation. *Development* **132:** 345–357.

Merchán P, Bribián A, Sánchez-Camacho C, Lezameta M, Bovolenta P, de Castro F. 2007. Sonic hedgehog promotes the migration and proliferation of optic nerve oligodendrocyte precursors. *Mol Cell Neurosci* **36:** 355–368.

Münsterberg AE, Kitajewski J, Bumcrot DA, McMahon AP, Lassar AB. 1995. Combinatorial signaling by Sonic hedgehog and Wnt family members induces myogenic bHLH gene expression in the somite. *Genes Dev* **9:** 2911–2922.

Otto A, Schmidt C, Patel K. 2006. Pax3 and Pax7 expression and regulation in the avian embryo. *Anat Embryol* **211:** 293–310.

Petrie RJ, Doyle AD, Yamada KM. 2009. Random versus directionally persistent cell migration. *Nat Rev Mol Cell Biol* **10:** 538–549.

Polizio AH, Chinchilla P, Chen X, Kim S, Manning DR, Riobo NA. 2011. Heterotrimeric Gi proteins link Hedgehog signaling to activation of Rho small GTPases to promote fibroblast migration. *J Biol Chem* **286:** 19589–19596.

Pouthas F, Girard P, Lecaudey V, Ly TB, Gilmour D, Boulin C, Pepperkok R, Reynaud EG. 2008. In migrating cells, the Golgi complex and the position of the centrosome depend on geometrical constraints of the substratum. *J Cell Sci* **121:** 2406–2414.

Pownall ME, Gustafsson MK, Emerson CP Jr. 2002. Myogenic regulatory factors and the specification of muscle progenitors in vertebrate embryos. *Annu Rev Cell Dev Biol* **18:** 747–783.

Purcell P, Joo BW, Hu JK, Tran PV, Calicchio ML, O'Connell DJ, Maas RL, Tabin CJ. 2009. Temporomandibular joint formation requires two distinct hedgehog-dependent steps. *Proc Natl Acad Sci* **106:** 18297–18302.

Ray RS, Corcoran AE, Brust RD, Kim JC, Richerson GB, Nattie E, Dymecki SM. 2011. Impaired respiratory and body temperature control upon acute serotonergic neuron inhibition. *Science* **333:** 637–642.

Rees E, Young RD, Evans DJR. 2003. Spatial and temporal contribution of somitic myoblasts to avian hind limb muscles. *Dev Biol* **253:** 264–278.

Renault M-A, Roncalli J, Tongers J, Thorne T, Klyachko E, Misener S, Volpert OV, Mehta S, Burg A, Luedemann C, et al. 2010. Sonic hedgehog induces angiogenesis via Rho kinase-dependent signaling in endothelial cells. *J Mol Cell Cardiol* **49:** 490–498.

Riddle R, Johnson R, Laufer E, Tabin C. 1993. Sonic hedgehog mediates the polarizing activity of the ZPA. *Cell* **75:** 1401–1416.

Sasaki N, Kurisu J, Kengaku M. 2010. Sonic hedgehog signaling regulates actin cytoskeleton via Tiam1–Rac1 cascade during spine formation. *Mol Cell Neurosci* **45:** 335–344.

Scaal M, Gros J, Lesbros C, Marcelle C. 2004. In ovo electroporation of avian somites. *Dev Dyn* **229:** 643–650.

Schiaffino S, Reggiani C. 1996. Molecular diversity of myofibrillar proteins: Gene regulation and functional significance. *Physiol Rev* **76:** 371–423.

Serrador JM, Nieto M, Sánchez-Madrid F. 1999. Cytoskeletal rearrangement during migration and activation of T lymphocytes. *Trends Cell Biol* **9:** 228–233.

Shubin NH, Alberch P. 1986. A morphogenetic approach to the origin and basic organization of the tetrapod limb. *Evol Biol* **20:** 319–387.

Shubin NH, Daeschler EB, Jenkins FA. 2006. The pectoral fin of *Tiktaalik roseae* and the origin of the tetrapod limb. *Nature* **440:** 764–771.

Sordino P, van der Hoeven F, Duboule D. 1995. Hox gene expression in teleost fins and the origin of vertebrate digits. *Nature* **375:** 678–681.

Tajbakhsh S, Buckingham M. 2000. The birth of muscle progenitor cells in the mouse: Spatiotemporal considerations. *Curr Top Dev Biol* **48:** 225–268.

Thorsen DH, Hale ME. 2005. Development of zebrafish (*Danio rerio*) pectoral fin musculature. *J Morphol* **266:** 241–255.

van den Heuvel M, Ingham PW. 1996. smoothened encodes a receptor-like serpentine protein required for hedgehog signalling. *Nature* **382:** 547–551.

Van Swearingen J, Lance-Jones C. 1995. Slow and fast muscle fibers are preferentially derived from myoblasts migrating into the chick limb bud at different developmental times. *Dev Biol* **170:** 321–337.

Wagner GP, Chiu CH. 2001. The tetrapod limb: A hypothesis on its origin. *J Exp Zool* **291:** 226–240.

Wigmore PM, Evans DJR. 2002. Molecular and cellular mechanisms involved in the generation of fiber diversity during myogenesis. *Int Rev Cytol* **216:** 175–232.

Williams BA, Ordahl CP. 1994. Pax-3 expression in segmental mesoderm marks early stages in myogenic cell specification. *Development* **120:** 785–796.

Yam PT, Langlois SD, Morin S, Charron F. 2009. Sonic hedgehog guides axons through a noncanonical, Src-family-kinase-dependent signaling pathway. *Neuron* **62:** 349–362.

Yang Y, Guillot P, Boyd Y, Lyon MF, McMahon AP. 1998. Evidence that preaxial polydactyly in the Doublefoot mutant is due to ectopic Indian Hedgehog signaling. *Development* **125:** 3123–3132.

Zhang XM, Ramalho-Santos M, McMahon AP. 2001. Smoothened mutants reveal redundant roles for Shh and Ihh signaling including regulation of L/R symmetry by the mouse node. *Cell* **106:** 781–792.

Supplemental Figures, Figure Legends, Tables, and Movie Legends

Supplemental Fig. 1

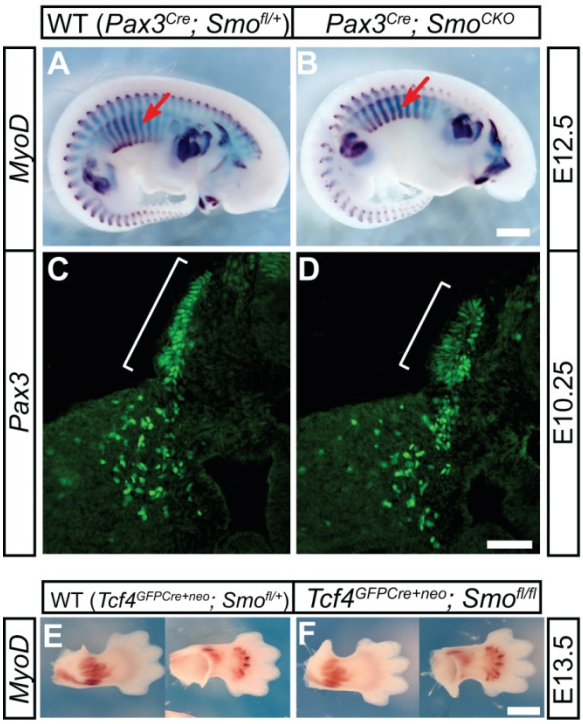

Supplemental Figure 1 (related to Figure 1). Shh activity is required cell-autonomously for normal somite morphology but its non-cell-autonomous action through muscle connective tissue is dispensable for later muscle formation. (A,B) *MyoD in situ* hybridization revealed that in the absence of Hh activity in the muscle progenitor cells, the myotome was shortened at E12.5 (red arrows). (C,D) Similarly, immunostaining using Pax3 antibody showed that the medial dermomyotome was malformed in the *Pax3^{Cre}; Smo^{CKO}* mutant at E10.25, leading to an overall shortened structure (compare the brackets). (E,F) *MyoD* hybridization showed that removal of Hh activity in the muscle connective tissue using *Tcf4 $^{GFPCre+neo}$* did not affect the development of limb muscles at E13.5. Bars: A and B, 1 mm; C and D, 300 μm; E and F, 1.6 mm.

Supplemental Fig.2

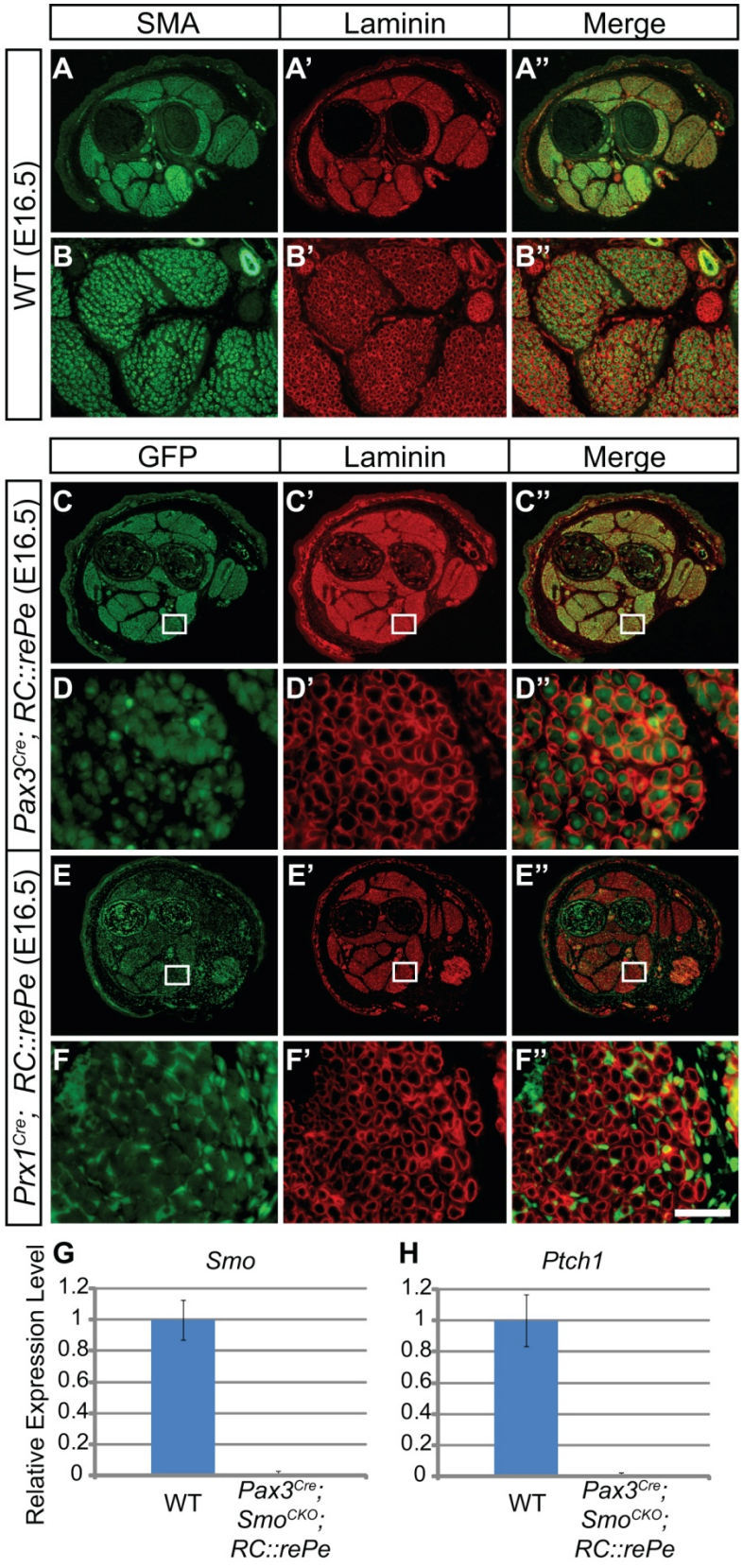

Supplemental Figure 2 (related to Figure 1). Colocalization of SMA, laminin, and Cre-responsive GFP reporter. (A-B") Frozen sections of E16.5 mouse forelimbs at the zeugopod level were immunostained for smooth muscle actin (SMA) (A and B) and laminin (A' and B'), which were co-localized in the skeletal muscle bundles (A" and B"). (C-F") Similar sections from embryos that carried $Pax3^{Cre}$ (C-D") or $Prx1^{Cre}$ (E-F") and a Cre-responsive GFP reporter (*RC::rePe*) were immunostained for GFP and laminin. GFP expression showed that $Pax3^{Cre}$ activity was confined within the limb muscles (C" and D") and $Prx1^{Cre}$ activity was specific for non-muscle limb tissues (E" and F"). (G,H) $Pax3^{Cre}$ effectively removed *Smo* alleles in the $Pax3^{Cre}$*; Smo*^{CKO}*; RC::rePe* mutant muscle progenitors at E10.75 (G), which were collected by FACS sorting. This led to the removal of cell-autonomous Hh activity in the Pax3 descendents, as assessed by *Ptch1* expression at E10.75 (H). Both *Smo* and *Ptch1* expression levels were measured by qPCR and normalized to β-actin expression. Bar in F" corresponds to 400 μm in A-A", C-C", and E-E", 100 μm in B-B", and 35 μm in D-D" and F-F".

Supplemental Fig. 3

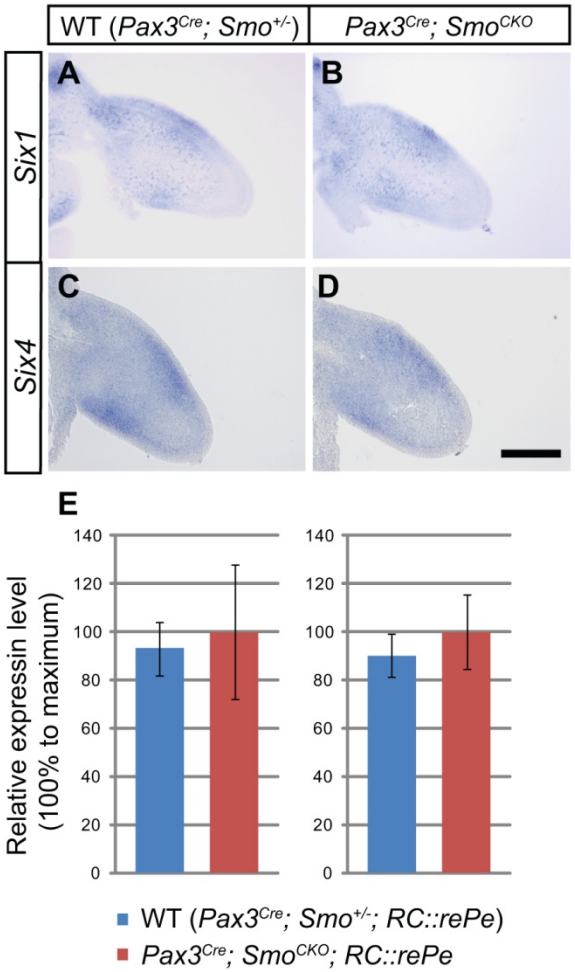

Supplemental Figure 3 (related to Figure 3). *Six1* and *Six4* expression was unaffected in the *Pax3^{Cre}; Smo^{CKO}* mutant forelimb muscle cells. (A-E) The expression of Six1/4 at E10.5 was analyzed by section *in situ* hybridization (A-D) and Qpcr (E). No change in their expression level was observed. Histograms are expressed as means and standard error of the mean (SEM) (n = 3 for each genotype). Bar in D corresponds to 200 μm in A-D.

Supplemental Fig. 4

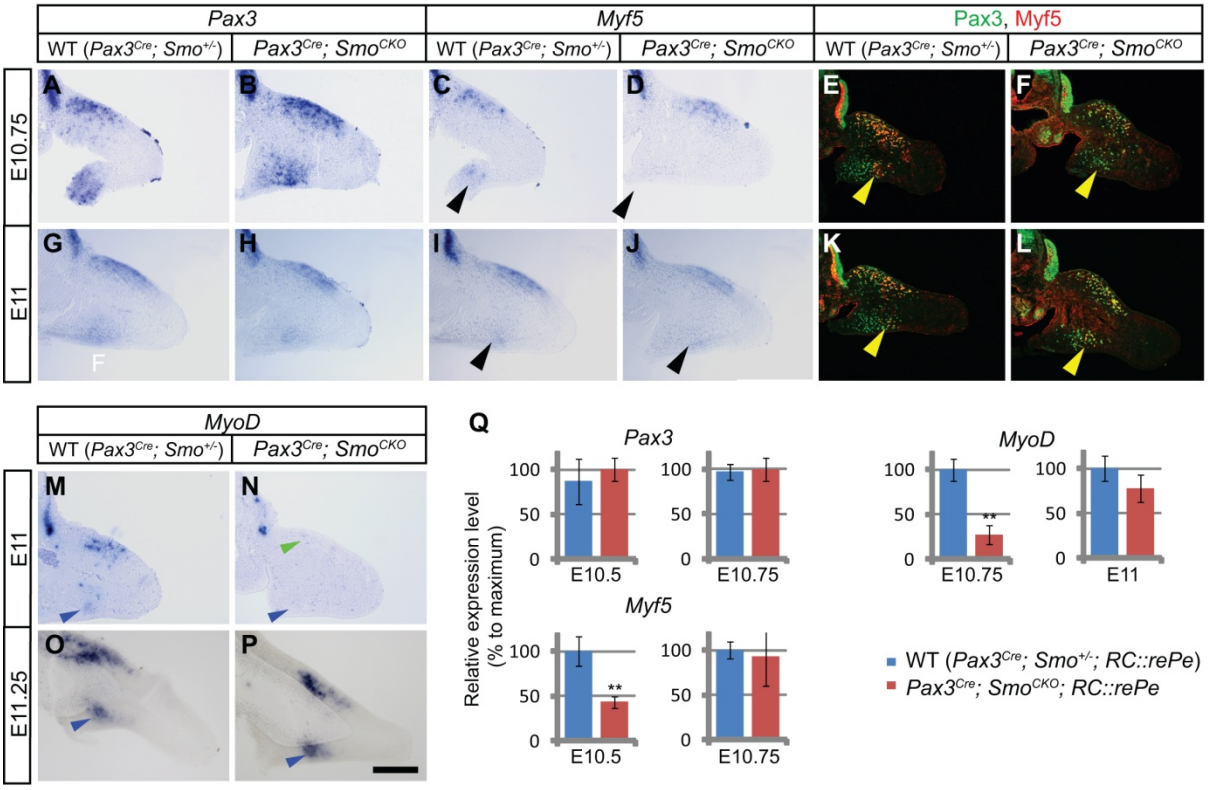

Supplemental Figure 4 (related to Figure 3). The initiation of the myogenic program is delayed in the *Pax3^{Cre}; Smo^{CKO}* mutant hindlimb ventral muscle cells. (A-D) When Hh signaling is removed cell-autonomously from muscle progenitor cells, section *in situ* hybridization showed that at E10.75 the initiation of *Myf5* expression was delayed in the *Pax3^{Cre}; Smo^{CKO}* mutant hindlimb ventral muscle cells (C,D, black arrowheads). However, *Pax3* expression was unaffected (A,B). (E,F) Similar observation (yellow arrowhead) was made by using antibodies against Myf5 (red) and Pax 3 (green), (G-L) At E11, however, *Myf5* expression had recovered (black and yellow arrowheads). (M-P) Like *Myf5*, the initiation of *MyoD* expression was delayed in the *Pax3^{Cre}; Smo^{CKO}* mutant hindlimb muscle cells at E11, as assessed by *in situ* hybridization (M and N, blue arrowheads). In the most severe case, even the dorsal muscle mass was affected (green arrowhead). However, by E11, the expression of *MyoD* was restored (O,P). (Q) To confirm the expression of *Pax3*, *Myf5*, and *MyoD*, a Cre-responsive GFP reporter (*RC::rePe*) was used to

generate GFP positive muscle cells for FACS sorting. Myogenic cells from the ventral hindlimb were isolated and analyzed by qPCR, which further demonstrated that the initiation of *Myf5* and *MyoD* expression was delayed in the $Pax3^{Cre}; Smo^{CKO}$ mutant ventral limb muscle, but recovered to almost WT levels at a later stage. Expression levels were normalized to GAPDH expression. Histograms are expressed as means and standard error of the mean (SEM) (n = 3 for each genotype). ***$p < 0.001$, *$p<0.05$. Bar in P corresponds to 200 μm in A-P.

Supplemental Fig. 5

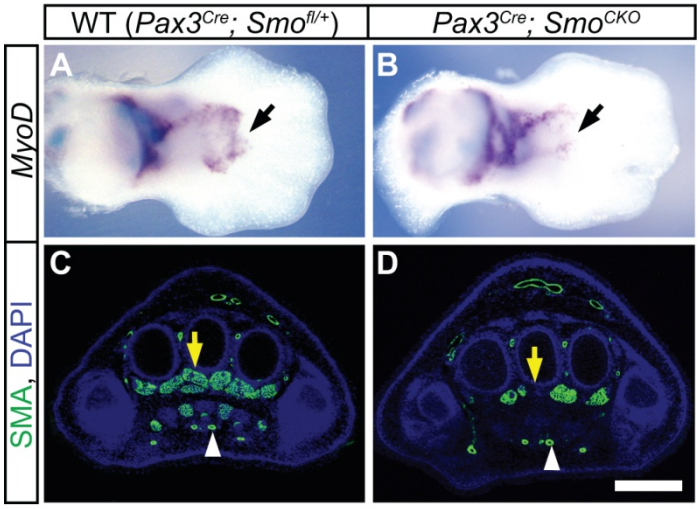

Supplemental Figure 5 (related to Figure 4). Cell-autonomous Shh activity is required for distal muscle formation in the hindlimb. (A,B) *MyoD* expression in the E12.5 ventral hindlimbs revealed that, similar to the forelimb, there was a reduced myogenic population in the mutant autopod (black arrows), where Hh signaling had been removed from muscle progenitor cells. (C,D) This reduction led to a partial loss of muscles in the *Pax3*^{Cre}*; Smo*^{CKO} mutant feet at E16.5 (yellow arrows), as assessed by SMA immunostaining. However, blood vessels were unaffected (white arrowheads). Bar: A and B, 500 µm; C and D, 400 µm.

Supplemental Fig. 6

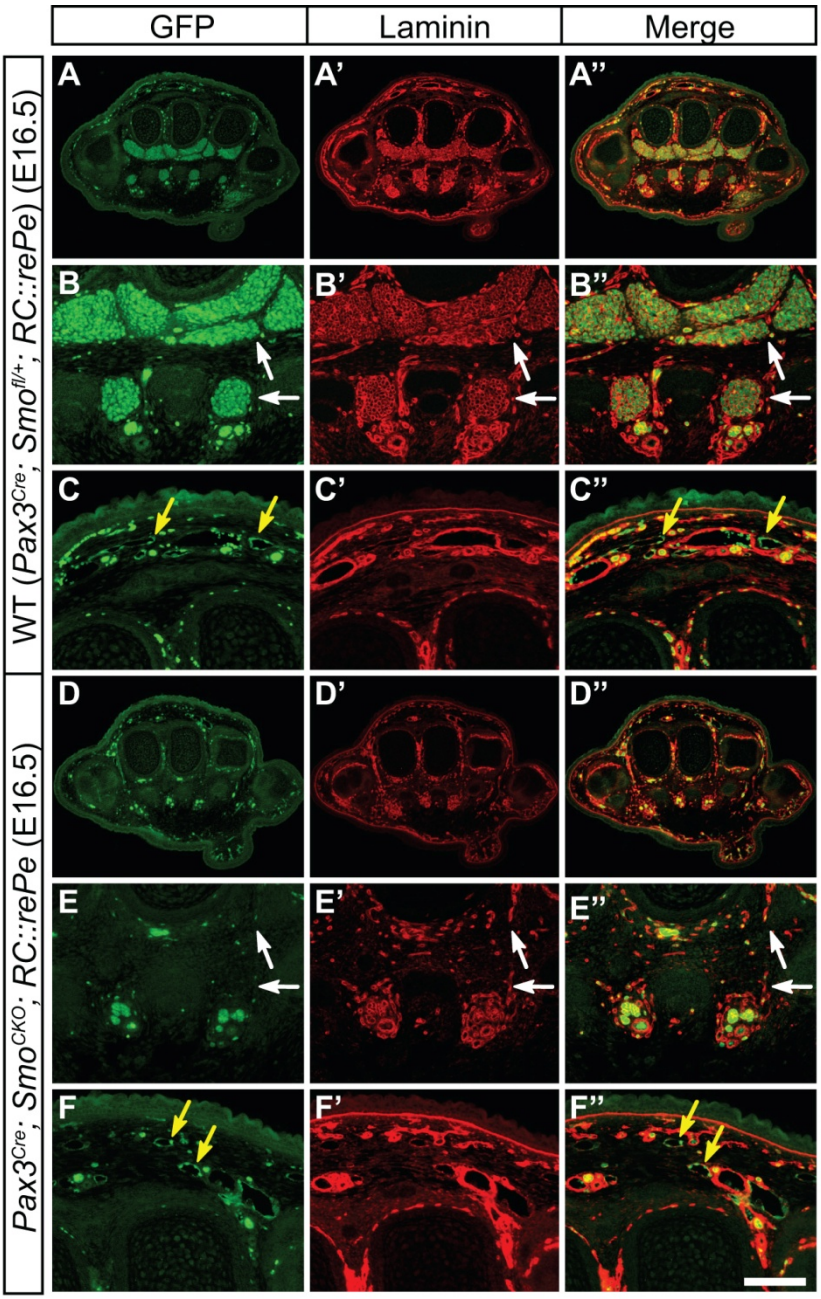

Supplemental Figure 6 (related to Figure 4). Shh is required cell-autonomously for distal muscle formation, but dispensable for distal blood vessels. (A-F") Frozen sections of E16.5 WT (A-C") and *Pax3^{Cre}; Smo^{CKO}; RC::rePe* mutant forelimbs (D-F") were immunostained for GFP and laminin. (B-C")

are enlargements of (A-A”) and (E-F”) are enlargements of (D-D”). GFP positive *Pax3*-myogenic descendents were absent in mutant limbs, where Hh activity had been removed from muscle progenitor cells (white arrows). However, *Pax3* endothelial descendents were still present in the autopod and were not affected by cell-autonomous loss of Hh signaling (yellow arrows). Bar in F” corresponds to 400 μm in A-A” and D-D”, and 100 μm in B-C” and E-F”.

Supplemental Fig. 7

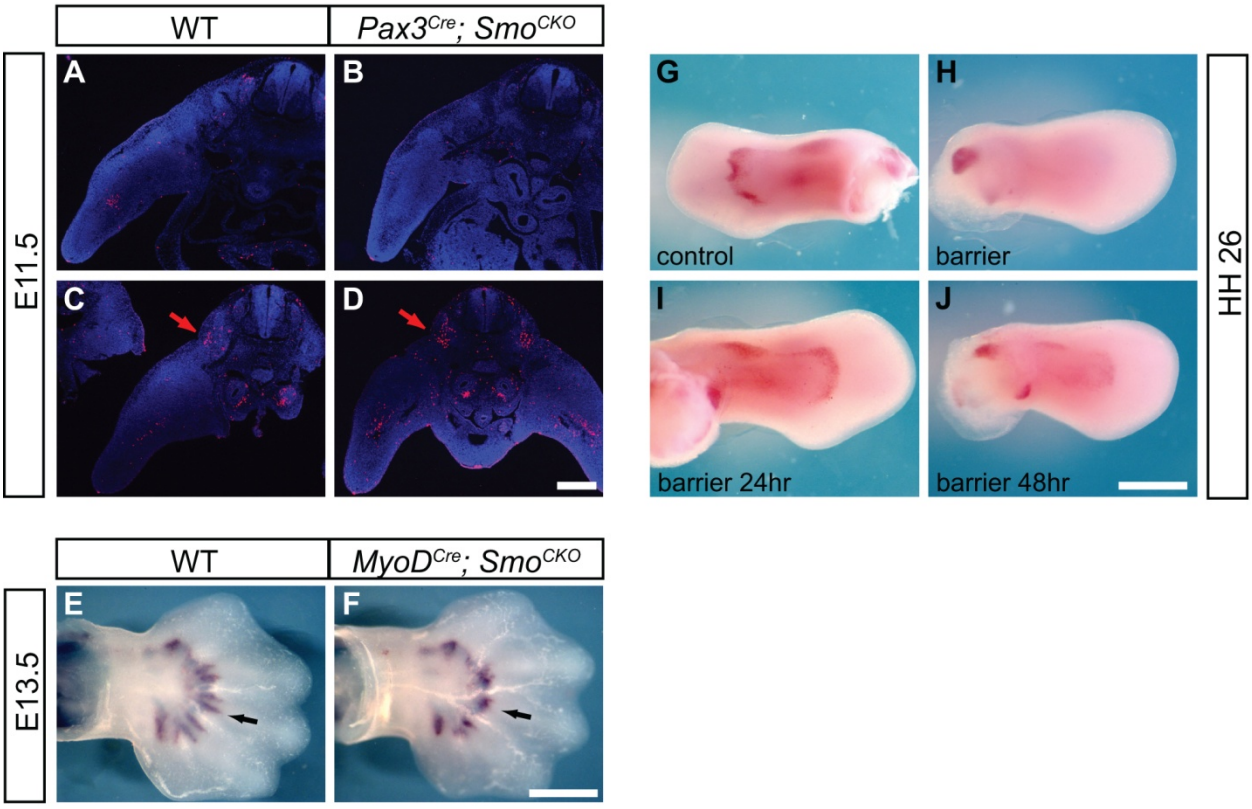

Supplemental Figure 7 (related to Figure 5). Early apoptosis in the dermomyotome is not the cause of the loss of distal limb muscles. (A-D) TUNEL staining (red) of E11.5 WT embryos (A,C) and *Pax3*^{Cre}*; Smo*^{CKO} mutant siblings (B,D) showed no increase of apoptosis in tissues at the forelimb level (A,B). However, there was an increase in apoptosis in the dermomyotome at the hindlimb level (C,D, red arrows). (E and F) When *Smo* was removed in myocytes using MyoD^{Cre}, *MyoD in situ* showed distal truncation in the autopod muscles when compared to the WT limb (black arrows). (G-J) In the chick system, when a metal barrier was placed between the somites and the forelimb, ventral muscles failed to form because of the blockage, as assessed by *Myf5 in situ* hybridization (H). However, if the barriers were removed after either 24 or 48 hours, distal muscles did form, although there was less muscle if the barrier was removed at a later stage (I,J). Bars: A-D, 300 μm; E and F, 500 μm; G-J, 1 mm.

Supplemental Fig. 8

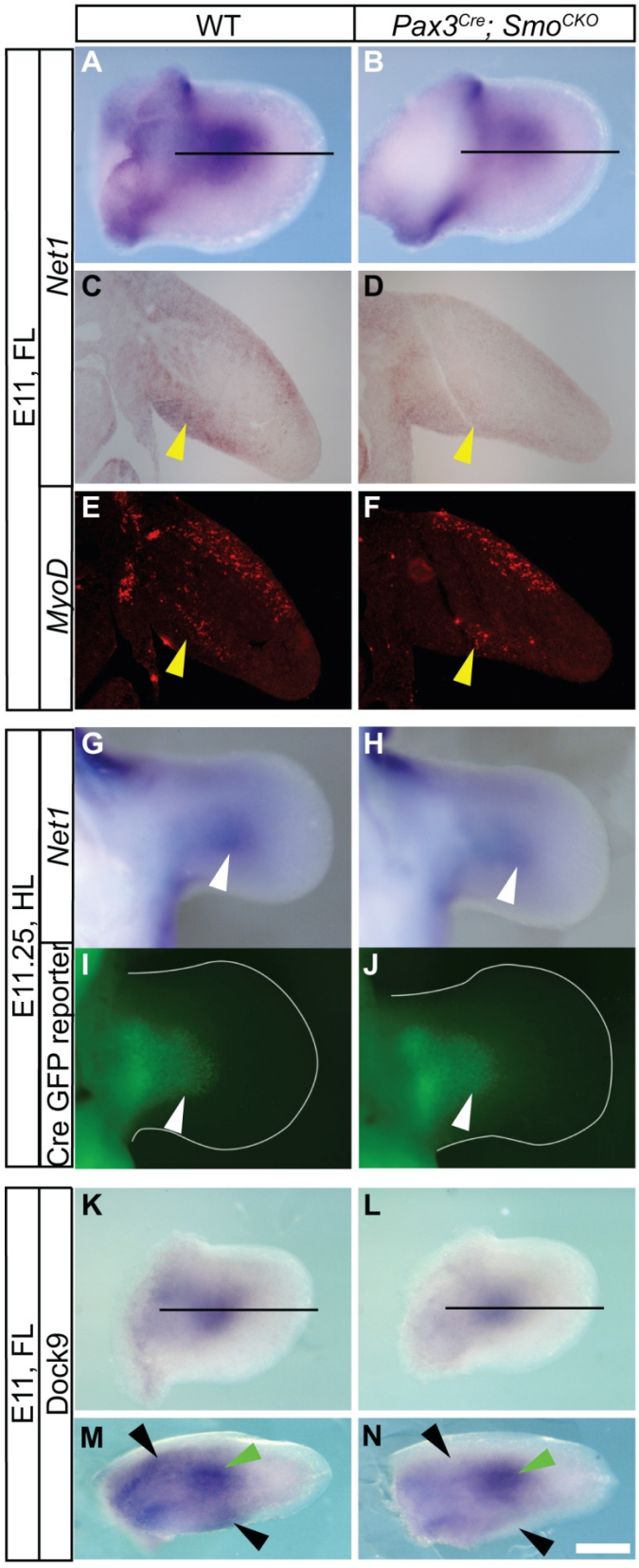

Supplemental Figure 8 (related to Figure 7). Hh signaling is required cell-autonomously to maintain *Net1* and *Dock9* expression. (A,B) *Net1* whole mount *in situ* hybridization on E11 mouse limbs showed that *Net1* is downregulated in the $Pax3^{Cre}; Smo^{CKO}$ mutant limb. (C,D) Similarly, *Net1* section *in situ* at the level indicated by the black lines in (A,B) also revealed reduced *Net1* expression in the mutant limb. (E,F) This loss of *Net1* expression, however, was not due to a loss in myocytes, marked by *MyoD* probe on the same section (yellow arrowheads). (G-J) *Net1 in situ* hybridization showed that *Net1* expression was downregulated in the $Pax3^{Cre}; Smo^{CKO}; RC::rePe$ mutant hindlimb (H, white arrowhead) at E11.25 when compared to the WT limb bud (G). This downregulation was not due to a loss of muscle progenitors in the limb, marked by $Pax3^{Cre}$ responsive GFP reporter (I,J). (K-N) *Dock9* expression in the muscles was also downregulated in the $Pax3^{Cre}; Smo^{CKO}$ mutant limb. By clipping the limb at the level indicated by the black lines in (G,H), *Dock9* expression, as observed from the lateral side, was found in the condensing mesenchyme (green arrowheads) and both of the dorsal and ventral muscle masses (black arrows) in the WT limb. While its expression in the cartilage was unaffected, it was downregulated in the ventral limb muscle. Bar in N corresponds to 250 μm in A, B, G-J, M, and N, 150 μm in C-F, and 200 μm in K and L.

Supplemental Tables

Supplemental Table 1

Genes	**Forward**	**Reverse**
Pax3 (91bp)	TACCAGCCCACGTCTATTCCACAA	TTTGGTGTACAGTGCTCGGAGGAA
Six1 (94bp)	ACCGGAGGCAAAGAGACC	GGAGAGAGTTGATTCTGCTTGTT
Six4 (169bp)	GGCATTGTCCAGATCCCTAA	CTGTGGCTGGCTCACTTGTA
Myf5 (198bp)	TGAGGGAACAGGTGGAGAAC	AGCTGGACACGGAGCTTTTA
MyoD (201bp)	AGCACTACAGTGGCGACTCA	GCTCCACTATGCTGGACAGG
Smo (93bp)	TTGTGCTCATCACCTTCAGC	TGGCTTGGCATAGCACATAG
Ptch1 (144bp)	ATCTCGAGACCAACGTGGAG	TAGCGCCTTCTTCTTTTGGA
GAPDH (104bp)	CATGGCCTTCCGTGTTCCTA	CCTGCTTCACCACCTTCTTGAT
β-actin (134bp)	GGCACCACACYTTCTACAATG	GGGGTGTTGAAGGTCTCAAAC

Supplemental Table 1 (related to Materials and Methods). Primer sets for qPCR.

Supplemental Table 2

Antibody	Source	Product number	Sample preparation	Dilution	Block	NaCitrate antigen retrieval
mouse anti-alpha smooth muscle actin	abcam	ab8211	Paraffin	1:100	1% BSA + 10% GS	works with and without
rabbit anti-laminin	Sigma	L-9393	Frozen or paraffin	1:100	1% BSA + 10% GS	works with and without
mouse anti-slow skeletal (type I) myosin	Sigma	M8421 (NOQ7.5.4D)	Frozen	1:500	1% BSA + 10% GS	yes
chick anti-GFP	abcam	ab13970	Frozen	1:500	1% BSA + 10% GS	no
			Paraffin	1:2000		yes
mouse anti-Pax3	R&D Systems	MAP2457	Frozen	1:50	1% BSA + 10% GS	no
			Paraffin	1:50		yes
mouse anti-Pax7	DSHB	Pax7	Frozen	1:10	1% BSA + 10% GS	no
rabbit anti-cleaved caspase-3	Cell Signaling	9661	Paraffin	1:100	1% BSA + 10% GS	yes
rabbit anti-phosphohistone H3	Millipore	06-570	Paraffin	1:100	1% BSA + 10% GS	yes
rabbit anti-GM130	abcam	ab52649	Paraffin	1:250	1% BSA + 10% GS	yes
rabbit anti-Myf5	Santa Cruz	sc-302	Frozen (4% PFA for 30 minutes	1:1500	1% BSA + 10% GS	no
mouse anti-MyoD	Santa Cruz	sc-32758	Frozen (0.5% PFA for 30 minutes)	1:200	1% BSA + 1% GS	no
mouse anti-GST	Invitrogen	13-6700	Frozen	1:100	1% BSA	no

Supplemental Table 2 (related to Materials and Methods). A list of all the primary antibodies that were used in this paper. All antibodies were diluted in the block listed without GS. BSA, bovine serum albumin; GS, goat serum

Supplemental Movies

Supplemental Movie 1 (related to Figure 5). In the presence of Shh protein, chick primary muscle cells efficiently migrated over the scratch to close the wound.

Supplemental Movie 2 (related to Figure 5). When Hh signaling was blocked by cyclopamine, chick primary muscle cells continued to move, but failed to close the scratched gap.

Supplemental Movie 3 (related to Figure 5). In the presence of Shh protein, mouse primary muscle cells efficiently migrated over the scratch to close the wound.

Supplemental Movie 4 (related to Figure 5). When Hh signaling was blocked by cyclopamine, mouse primary muscle cells continued to move, but failed to close the scratched gap.

Supplemental Movie 5 (related to Figure 5). At E11, ventral limb muscle cells in the WT embryos migrated distally over a period of 7.5 hours.

Supplemental Movie 6 (related to Figure 5). At E11, ventral limb muscle cells failed to migrate distally when Hh activity was removed from muscle progenitor cells. Occasionally, a few cells did migrate distally, but they often retracted at the end.